

Sine-Liouville gravity as a Vertex Model on Planar Graphs

Ivan Kostov ^{a,b}

^a *Université Paris-Saclay, CNRS, CEA, Institut théorique
91191 Gif-sur-Yvette, France*

^b *Beijing Institute of Mathematical Sciences and Applications
Huairou 101408, Beijing, China*

E-mail: ivan.kostov@ipht.fr

ABSTRACT: We investigate the universal behaviour of a one-parameter generalisation of the six-vertex model on planar graphs, which we refer to as the seven-vertex (7v) model. The 7v model is characterised by a temperature coupling and its continuum limit exhibits massive, dilute and dense phases similarly to the $O(n)$ loop model. However, there is an important distinction: the loop weights are no longer topological and the dynamics of the loops is now entangled with the local geometry of the lattice. We compute the sphere and disk partition functions of the 7v model from the spectral curve of the dual matrix model. The disk partition function for fixed length is a deformation of the Bessel integral known as the Krätzel function. We argue that the 7v matrix model and Matrix Quantum Mechanics provide two complementary non-perturbative realisations of sine-Liouville gravity. Specifically, we find that the continuum limits of 7vMM and MQM share the same classical spectral curve but describe two different types of branes in sine-Liouville gravity. The 7vMM precisely covers the range of parameters where the Minkowskian MQM lacks a simple interpretation in terms of multiple tachyon scattering. We investigate the flow relating the dilute and dense phases and argue that this flow is the gravitational analogue of the massless flow in the sine-Gordon model with imaginary mass coupling. The two endpoints of the flow are described by a free boson coupled to Liouville gravity and compactified on circles with two different radii.

In memory of Ivan Todorov

Contents

1	Introduction and summary of the results	1
2	Sine-Liouville gravity	5
2.1	Sine-Gordon QFT	5
2.2	Sine-Liouville gravity	7
3	The 7-vertex model on planar graphs	8
3.1	Definition and loop expansion	8
3.2	The 7-vertex matrix model	11
3.3	Collective field and Virasoro constraint	13
4	Thermodynamical limit and spectral curve	15
4.1	Boundary value problem	15
4.2	Phase diagram and scaling limit	16
4.3	Uniformisation of the boundary value problem in the scaling limit	17
4.4	Solution at the critical point ($M = 0$)	18
4.5	Solution of the boundary value problem in the continuum limit	19
4.6	Computation of the boundary entropy	20
4.7	Partition function on the sphere and susceptibility	20
4.8	UV and IR compactification radii	22
4.9	Boundary length distribution	22
5	Relation to Matrix Quantum Mechanics and 2D string theory	23
5.1	The classical spectral curve of MQM	23
5.2	7vMM versus MQM	25
6	Discussion	27

1 Introduction and summary of the results

Sine-Liouville gravity, or sine-Gordon model coupled to 2D gravity, is a rich and fascinating theory. Although it has been studied for more than three decades, starting with [1, 2], some aspects of the theory, especially concerning the boundary behaviour, are still poorly understood.

The sine-Liouville gravity is closely related to the sine-Liouville CFT which, according to the Fateev-Zamolodchikov-Zamolodchikov (FZZ) conjecture [3, 4] proved rigorously in [5], is mapped by strong/weak coupling duality to the Euclidean black hole (cigar) CFT [6, 7]. A non-perturbative description of the sine-Liouville gravity is provided by Matrix Quantum Mechanics (MQM) [8–11] perturbed by a source of winding [12] or momentum [13]

modes. The perturbed MQM exhibits Toda integrability, first discovered in [14] and then exploited to investigate different aspects of the 2D string theory: winding mode [12] and momentum mode [13, 15] condensates, and non-perturbative effects due to sine-Liouville instantons [16, 17].

In this paper we present an alternative holographic dual of Euclidean sine-Liouville gravity with a neat statistical interpretation. Our construction is based on the integrable lattice regularisation of the sine-Gordon quantum field theory by the *honeycomb seven-vertex model*.¹ This vertex model, first studied by Baxter [20, 21], gives a local formulation of the $O(n)$ model [22]. The local degrees of freedom of the vertex model are arrows assigned to the bonds of the honeycomb lattice obeying the “ice rule” that the numbers of incoming and outgoing arrows at each site must be equal. The ice rule allows seven arrow configurations at each vertex of the honeycomb lattice as shown in fig. 1. The local Boltzmann weights are associated with these seven vertex configurations, or simply vertices. Assuming invariance under $\pi/3$ rotations, which we must do when we consider dynamical lattices, there are only three distinct vertices which can be parametrised up to a common factor as

$$w_1 = T, \quad w_2 = w_3 = w_4 = w, \quad w_5 = w_6 = w_7 = w^{-1}. \quad (1.1)$$

The parameter T is sometimes referred to as the temperature coupling or shortly the temperature. Each vertex configuration defines a collection of self-avoiding and mutually avoiding oriented loops, and the partition sum of the vertex model is expanded as

$$Z = (T)^{\text{sites}} \sum_{\text{oriented loops}} (1/T)^{(\text{occupied sites})} w^{(\text{left turns}) - (\text{right turns})}. \quad (1.2)$$

Since on the infinite lattice the number of the right turns differs from the number of the left turns by ± 6 , the loop expansion (1.2) is that of the $O(n)$ model with $n = w^6 + w^{-6}$ [22]. The 7v model is exactly solvable with the special choice for the temperature coupling $T_{\pm} = (2 \pm \sqrt{2 - n})^{1/2}$ [19–21, 23]. The loop gas exhibits nontrivial critical behavior when w is a unimodular complex number so that $|n| \leq 2$. Its phase diagram shows two critical phases, the phase of dilute loops at $T_c = T_+$ and the critical phase of dense loops at $T < T_c$ which includes the other solvable point T_- . The two critical phases correspond to the two renormalisation-group fixed points of the sine-Gordon theory with imaginary mass coupling and the massless flow connecting them was investigated in a series of papers by P. Fendley, H. Saleur and Al. Zamolodchikov [24–26].

The 7-vertex model has the advantage, compared to the other discretisations of the sine-Gordon model, that its weights are isotropic and therefore can be defined on any trivalent planar graph. Sometimes it is useful to represent the trivalent graph by its dual triangulation where we can define local curvature associated with the vertices of the triangulation. An example of a vertex configuration on a trivalent graph with the topology of a disk together

¹This statistical model has been given different names in the literature. We adopted the name “seven-vertex model” following Batchelor and Blöte [18]. We consider the formulation of the 7-vertex model in terms of arrows on a honeycomb lattice [19] because it is most naturally generalised to dynamical lattices.

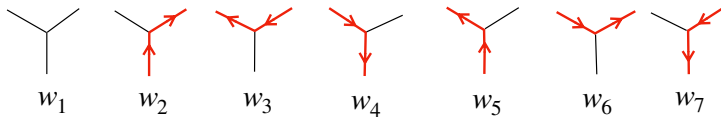


Figure 1. The vertices of the 7-vertex model.

with its dual triangulation is shown in fig. 2. Considering the ensemble of all trivalent planar graphs, we add the gravitational degrees of freedom to achieve an integrable lattice regularisation of the gravitational sine-Gordon model.

Again, the 7-vertex model on planar graphs can be reformulated as a gas of oriented self-avoiding and mutually avoiding loops and in this respect resembles the gravitational $O(n)$ loop model [27]. The dynamics is however quite different because the Boltzmann weights of the loops depend on the local curvature through an effective spin connection. In general, vertex models on planar graphs represent a separate and still unexplored niche of solvable models of 2D gravity, and can reveal new unexpected phenomena, especially in the case of lattices with boundaries.

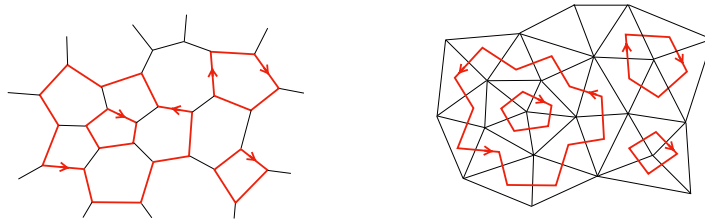


Figure 2. A loop configuration on a trivalent graph with the topology of the disk and on its dual triangulation. To preserve the information about the topology the lines should be thickened.

We solve the gravitational 7v model by mapping it to a large- N matrix model representing a one-parameter deformation of the 6-vertex matrix model formulated originally by Ginsparg [28] and solved in [29–31]. We will parametrise the vertices in fig. 1 in a way compatible with the conventions of [29] by setting in (1.1)

$$w = e^{i\pi\lambda/2}. \quad (1.3)$$

Interesting critical behaviour exists only for real λ . By the symmetries of the Boltzmann weights one can restrict $0 \leq \lambda < 1$. For $\lambda = 0$, the 7v matrix model is identical to the $O(2)$ matrix model [32].

In this paper, we are focusing on the universal behaviour in the scaling limit which is expected to be described by sine-Liouville gravity and which is characterised by two renormalised coupling constants, the cosmological constant μ and the temperature coupling t . In order to keep the parallel with MQM, we work in the grand canonical ensemble where the cosmological constant μ is defined as a chemical potential for N , see e.g. the review [33].

The grand partition function is a Fredholm determinant and can be viewed as an ensemble of free fermions with fixed Fermi energy μ . We formulate the Virasoro constraint on the spectral curve and solve it explicitly in the scaling limit, where the periodic cycle becomes infinite. The solution is unique up to renormalisation of the two coupling constants μ and t . The full solution of the matrix model will be reported in a forthcoming paper [34].

We will use at different places the parameters β , q and b related to the parameter $\lambda \in [0, 1]$ by

$$\boxed{\beta = \pi(1 + \lambda), \quad q = e^{i\beta}, \quad b = \sqrt{\frac{1-\lambda}{1+\lambda}}}. \quad (1.4)$$

With these conventions, the classical spectral curve in the scaling limit can be given the following parametric form, with λ considered as a continuous external parameter,

$$\begin{aligned} x &= M(\omega^b - \omega^{-1/b}), \\ y &= M^{1/b^2} \omega^{1/b} - t M^{b^2} \omega^{-b}. \end{aligned} \quad (1.5)$$

Here the quantity M is a function of μ and t determined by the (in general transcendental) equation

$$M^{1+\frac{1}{b^2}} - b^2 t M^{1+b^2} = (1 + b^2)\mu. \quad (1.6)$$

The meromorphic function $y(x)$ defined by eq. (1.5) determines the partition function on the disk with complexified boundary parameter x , and M is the boundary entropy generated by the fluctuations in the bulk of the disk. The observables depend on the couplings μ and t and are generally given, up to a power factor depending on their dimension, by scaling functions of the dimensionless variable $\hat{t} = t/\mu^{2\lambda/(1+\lambda)}$.

We derive the thermodynamical equation of state for the susceptibility $u(\mu, t) = \partial_\mu^2 \mathcal{F}_0$, where \mathcal{F}_0 is the partition function on the sphere,

$$\mu = \frac{1+\lambda}{2} e^{(1+\lambda)u} - \frac{1-\lambda}{2} t e^{(1-\lambda)u}. \quad (1.7)$$

This equation is a consequence of (1.6) and the relation between the boundary entropy and the susceptibility

$$M^2 = e^{(1-\lambda^2)u}. \quad (1.8)$$

The equation of state (1.7) has three critical points $t = 0, t \rightarrow -\infty$ and $t = t_c > 0$ corresponding to the dilute, the dense and the massive phases of the loop gas. As expected, the phase diagram of the 7v model matches the phase diagram of the sine-Gordon model on the plane where we observe two nontrivial and one trivial fixed point of the renormalisation group. The role of the scale parameter is played in sine-Liouville gravity by the cosmological constant μ which determines the size of the two-dimensional universe. The limit of large μ , or equivalently small t , describes the UV limit of the matter field which is that of a free compactified boson. When t becomes large and negative, the effective cosmological constant $-\mu/t$ diminishes and eq. (1.7) describes the physics at large distances. The second critical

point $t \rightarrow -\infty$ thus corresponds to the IR fixed point of the sine-Gordon model with *imaginary* mass coupling $\sim \sqrt{t}$. The transcendental equation (1.7) is the counterpart in sine-Liouville gravity of the massless flow in the sine-Gordon model with imaginary mass coupling studied in [24–26]. Finally, the third critical point $t = t_c$ is that of pure gravity and corresponds to the massive phase.

We find that at $t = 0$ and $t \rightarrow -\infty$ the matter field is that of a free boson compactified at radii respectively $R_{\text{UV}}^{\text{SL}}$ and $R_{\text{IR}}^{\text{SL}}$ related to the parameter λ of the 7-vertex model as

$$R_{\text{UV}}^{\text{SL}} = \frac{1 + \lambda}{2}, \quad R_{\text{IR}}^{\text{SL}} = \frac{1 - \lambda}{2}. \quad (1.9)$$

In our conventions, the self-dual radius is 1.

As expected, the equation of state (1.7) coincides with that of MQM [12, 13, 35]. Thus, restricting to the bulk observables, we find two different non-perturbative realisations of the same worldsheet theory. On the other hand, the boundary observables in the two theories are *different* because the two models correspond to two different Riemann surfaces sharing the same spectral curve. In MQM, the boundary observables for a given boundary length are expressed, at least for $t = 0$ and for $t \rightarrow -\infty$, in terms of Bessel- K functions. On the other hand, in 7vMM the boundary observables are expressed in terms of a generalised Bessel integral also known as the Krätzel function [36].

The plan of the paper is as follows. We start by reviewing in sect. 2 the phase structure of the sine-Gordon model and sine-Liouville gravity. In sect. 3 we define the partition function of the vertex model and derive its representations in terms of a gas of oriented loops on planar graphs and as an interaction-round-a-triangle height model. Then we formulate the dual large- N matrix model and derive the Dyson-Schwinger equations as a Virasoro constraint for a collective bosonic field. In sect. 4 we formulate the classical Virasoro constraint as a boundary value problem, obtain the solution at the critical point and in the continuum limit, and derive the partition functions on the sphere and on the disk. For the latter we give expressions both for fixed boundary parameter and for fixed boundary length. In sect. 5 we explain how the spectral curve of 7vMM compares to that of MQM and the consequences of the new understanding of the phase diagram for the proposal of [12] for an MQM-based description of the Euclidean “cigar” background.

2 Sine-Liouville gravity

2.1 Sine-Gordon QFT

We start by summarising the properties of the sine-Gordon model which we are going to use, such as the phase diagram, with the main purpose of fixing the notation. The sine-Gordon field theory can be viewed as a CFT of a free boson taking values in the circle of radius $1/2$, i.e. $\varphi + \pi \equiv \varphi$, and perturbed by a pair of exponential fields $e^{\pm 2i\varphi}$. The action for Euclidean signature is

$$\mathcal{A}_{SG}[\varphi] = \int \frac{g}{4\pi} (\partial_\mu \varphi)^2 + \mu_+ \int d^2x e^{2i\varphi} + \mu_- \int d^2x e^{-2i\varphi}. \quad (2.1)$$

The constant g is usually referred to as the Coulomb gas coupling because of the interpretation of the partition function as a gas of positive and negative charges [22]. The connection with the traditional notation is

$$g = \frac{8\pi}{\beta_{\text{SG}}^2}, \quad \mu_+ = \mu_- = \frac{m^2}{2\beta_{\text{SG}}^2}. \quad (2.2)$$

In terms of another commonly used parameter p , the CG coupling is written as

$$g = 1 + 1/p \quad (2.3)$$

Because of charge conservation, the bulk observables depend only on the product

$$t = \mu_+ \mu_-. \quad (2.4)$$

We are concerned here only with the regime $1 < g < 2$ where the sine-Gordon interaction is repulsive and the perturbation in the UV action (2.1) is relevant. To stress that g characterises the UV limit, sometimes we will denote $g = g_{\text{UV}}$. For real couplings μ_{\pm} , the renormalisation group (RG) analysis gives [37]

$$\partial_r \mu_{\pm} = \left(2 - \frac{2}{g}\right) \mu_{\pm}, \quad \partial_r \log g = 8\pi^2 \mu_+ \mu_- \quad (2.5)$$

where r is the rescaling parameter. By the first equation the coupling constants μ_{\pm} increase along the RG flow, by the second equation the Coulomb gas coupling g grows, which makes the perturbation even more relevant. The renormalised values of μ_{\pm} grow faster, the positive and negative charges proliferate, and the sine-Gordon model flows to a trivial massive plasma phase.

On the other hand, as discovered by Nienhuis [22], if μ_{\pm} are *purely imaginary*, their absolute values initially increase under renormalisation according to the first RG equation. However, since their product is negative, by the second RG equation the Coulomb gas coupling $g = g_{\text{UV}}$ decreases and the perturbation becomes less relevant. As a result, the Coulomb gas rarefies in the IR and the SG model flows again to a Gaussian field, but with a smaller value of the coupling constant $g_{\text{IR}} < 1$, so that the perturbation becomes irrelevant. The effective central charge starts at $c_{\text{UV}} = 1$ in the UV region, oscillates once around this value and returns ultimately again to $c_{\text{IR}} = 1$ in the IR [24, 26]. Since for imaginary coupling the theory is not unitary, Zamolodchikov's c -theorem does not apply for this flow.

With the help of the RG equations (2.5), one can determine the coupling constant at the endpoint of the flow in the IR. In the UV, the dimensions of the perturbing operators $e^{\pm 2i\varphi}$ are

$$h = \bar{h} = \frac{1}{g} = \frac{p}{p+1}. \quad (2.6)$$

For small t , the SG perturbation can be considered as triggered by a neutral local operator with coupling constant (2.4) and conformal dimensions

$$h_{\text{SG}} = \bar{h}_{\text{SG}} = 2h - 1 = \frac{2-g}{g} = \frac{p-1}{p+1}. \quad (2.7)$$

For large p , the two RG equations (2.5) give [22, 24, 25]

$$\frac{dg}{dr} = 2 [(g-1)^2 - 1/p^2]. \quad (2.8)$$

There are two fixed points of this equation, $g_{\text{UV}} = 1 + 1/p$ and $g_{\text{IR}} = 1 - 1/p$.

Instead of the coupling g , one can speak of the compactification radius. Rescaling $\varphi \rightarrow \varphi/\sqrt{g}$, we have a CFT of a Gaussian field with $g = 1$ and compactified on a circle of radius $R = \frac{1}{2}\sqrt{g}$. The massless RG flow then relates two $c = 1$ CFTs of free boson with different compactification radii

$$R_{\text{UV}}^{\text{SG}} = \frac{1}{2}\sqrt{1+1/p}, \quad R_{\text{IR}}^{\text{SG}} = \frac{1}{2}\sqrt{1-1/p}. \quad (2.9)$$

The strong-weak coupling duality $g \rightarrow 4/g$ transforms $R \rightarrow 1/R$, normalisation here is such that the self-dual radius is $R_{s.d.} = 1$, and the two Berezinskii-Kosterlitz-Thouless radii are respectively $R_{\text{BKT}} = 1/2$ and $\tilde{R}_{\text{BKT}} = 2$. When $g = 1$, the perturbation is marginal and $R_{\text{IR}} = R_{\text{UV}} = R_{\text{BKT}}$.

There are convincing arguments, summarised in [24], to believe that the sine-Gordon model represents the effective quantum field theory describing the vicinity of the critical point T_c for the 7-vertex model, with the constant t proportional to the algebraic distance to critical value, $t \sim T - T_c$. The parameter p of the sine-Gordon interaction is related to the fugacity $n = w^6 + w^{-6}$ of the loop gas expansion by $n = 2 \cos(\pi/p)$. One can think of the oriented loops as kinks interpolating between adjacent classical vacua of the sine-Gordon potential. In the massive phase $T > T_c$ ($t > 0$), the theory falls into one of the vacua. Droplets of other classical vacua can appear but they are exponentially suppressed. At $T = T_c$ ($t = 0$), the kinks become massless and stay massless for $T < T_c$ ($t < 0$). For large negative t the kinks fill densely the lattice and form a critical phase.

2.2 Sine-Liouville gravity

Now let us turn to the sine-Liouville gravity, i.e. a theory of 2D gravity where the Euclidean sine-Gordon field plays the role of a matter field. This theory, also referred to as the gravitational sine-Gordon model, was first studied by G. Moore [1]. In conformal gauge for the gravitational field, the UV action depends on the sine-Gordon field φ and on the scale factor ϕ of the metric known as Liouville field. Given a background metric \hat{g}_{ab} with curvature \hat{R} , the UV action is²

$$\begin{aligned} \mathcal{A}_{\text{SL}}[\phi, \varphi] = & \frac{1}{4\pi} \int_{\mathcal{M}} d^2z \sqrt{\hat{g}} \left[(\hat{\nabla}\phi)^2 + (\hat{\nabla}\varphi)^2 + 2\phi\hat{R} \right] + \text{ghosts} \\ & + \mu \int d^2z \sqrt{\hat{g}} e^{2\phi} + \sum_{\pm} \mu_{\pm} \int d^2z \sqrt{\hat{g}} e^{(2-\frac{1}{R})\phi} e^{\pm \frac{i}{R}\varphi}. \end{aligned} \quad (2.10)$$

²We refer to the CFT defined by (2.10) as *sine-Liouville quantum gravity* in order to distinguish it from the *sine-Liouville conformal field theory*. In the latter there is no ghost sector, no Liouville potential, the marginal sine-Liouville interaction is $e^{\alpha\phi} \cos(a\varphi)$ with $a^2 - \alpha^2 = 2$, and the Liouville background charge is $Q = 1/\alpha$. If we ignore the ghost sector, then the sine-Liouville CFT and sine-Liouville QG intersect at $R = 2/3$ and $\mu = 0$. The FZZ conjecture [3, 4] states that the sine-Liouville CFT is related by strong/weak coupling duality to the ‘‘cigar’’ CFT with central charge $\frac{3k}{k-2} - 1$ [6, 7]. The mapping of the parameters is $a = \sqrt{k}$, $\alpha = \sqrt{k-2}$.

The exponents in the action are chosen so that the exponential operators are strictly marginal. Again, the path integral depends only on the product $t = \mu_+\mu_-$. A shift $\phi \rightarrow \phi + \log(r^2)$ is compensated by $\mu \rightarrow \mu/r^2$ and $\mu_{\pm} \rightarrow \mu_{\pm}/r^{\alpha}$ with $\alpha = 2 - 1/R$, so that the thermal coupling $t = \mu_+\mu_-$ scales as

$$t \sim \mu^{2-1/R}. \quad (2.11)$$

The phase diagram of sine-Liouville gravity is expected to be qualitatively the same as that of the sine-Gordon model in the plane. In particular, the massless flow in the sine-Gordon with imaginary mass coupling should have its counterpart in the sine-Liouville gravity. We will refer to it as *gravitational massless flow*.

The gravitational massless flow connects two theories of Liouville gravity with compactified boson as matter field. The parameter R in the UV action (2.10) is the compactification radius on the UV side, $R_{\text{UV}}^{\text{SL}} \equiv R$. The matter boson on the IR side has another compactification radius $R_{\text{IR}}^{\text{SL}}$. We will argue in section 4.8, based on the solution of the matrix model, that

$$R_{\text{IR}}^{\text{SL}} = 1 - R_{\text{UV}}^{\text{SL}}. \quad (2.12)$$

Another question one can ask is whether the compactification radius of the free boson is modified by switching on gravity and if so, what is the precise relation. In other words, is it possible to find a map f such that $R_{\text{UV}}^{\text{SL}} = f(R_{\text{UV}}^{\text{SG}})$ and $R_{\text{IR}}^{\text{SL}} = f(R_{\text{IR}}^{\text{SG}})$. Let us assume that such a map exists and it is the same for the UV and the IR CFTs. Comparing (2.12) and (2.9) written as

$$2(R_{\text{IR}}^{\text{SG}})^2 = 1 - 2(R_{\text{UV}}^{\text{SG}})^2, \quad (2.13)$$

we conclude that $f(x) = 2x^2 + \text{constant}$. The constant should be zero because at the BKT radius $R_{\text{IR}} = R_{\text{UV}} = 1/2$. Thus we arrive at the relation

$$2R_{\text{UV}}^{\text{SL}} = (2R_{\text{UV}}^{\text{SG}})^2, \quad 2R_{\text{IR}}^{\text{SL}} = (2R_{\text{IR}}^{\text{SG}})^2. \quad (2.14)$$

It makes sense to interpret this relation in terms of scaling dimensions because we cannot directly measure the radius but we can measure the dimension of the corresponding exponential field. On the rhs is the flat dimension of the exponential field $e^{\pm i\varphi/R^{\text{SG}}}$ while on the lhs is the so-called gravitational dimension [38–40] of the Liouville-dressed field $e^{\pm i\varphi/R^{\text{SL}}}$. The relation (2.14) tells us that the couplings μ_{\pm} scale with the same power of the volume before and after coupling to gravity.

3 The 7-vertex model on planar graphs

3.1 Definition and loop expansion

Starting with the discrete realisation of the sine-Gordon model by the 7v model, we construct, following [41–43], a discrete integrable realisation of sine-Liouville gravity by considering the 7v model in the ensemble of trivalent planar graphs.

Given the trivalent planar graph \mathcal{G} , the 7v degrees of freedom are introduced by assigning orientations to some of the bonds of \mathcal{G} in such a way that the number of the incoming and the outgoing arrows at each vertex is zero. Any such configuration gives rise to a set of loops on \mathcal{G} , and the partition function of the gas of loops takes the same form as (1.2).

The partition function of the gravitational 7v model on the sphere is then defined as a sum over all trivalent genus-zero planar graphs \mathcal{G} .

$$\begin{aligned}\mathcal{F}_0(\kappa, T) &= \sum_{\text{graphs } \mathcal{G}} \kappa^{V_{\mathcal{G}}} Z_{\mathcal{G}}(\kappa, T) \\ Z_{\mathcal{G}}(\kappa, T) &= \sum_{\text{loops } \mathcal{L} \text{ on } \mathcal{G}} (1/T)^{V_{\text{loops}}} \prod_{\mathcal{L}} w^{(\text{left turns}) - (\text{right turns})},\end{aligned}\tag{3.1}$$

where $w = \exp(\pi i \lambda / 2)$. Besides the temperature T coupled to the volume occupied by loops, V_{loops} , we introduce a new parameter κ , the “discrete cosmological constant”, coupled to the total volume of the graph $V_{\mathcal{G}}$. We will refer to the statistical model defined by (3.1) as the seven-vertex model on dynamical lattice or simply as the gravitational 7v model. The above definition is generalised in an obvious way to the case of planar graphs with boundaries and of higher genus. For graphs with a boundary, we have to introduce also a “discrete boundary cosmological constant” coupled to the boundary length.

The principal distinction between the loop expansions of the 7v model on a flat and on a dynamical lattice is that in the second case the fugacities of the loops are no longer topological: the dynamics of the loops is now entangled with the local geometry of the lattice. The consequences of the curvature defects for the loop gas have been elucidated by O. Foda and B. Nienhuis [44].

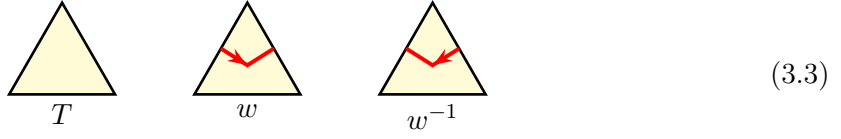
An alternative formulation of the gravitational 7v model is as an SOS type *height model* on dynamical triangular lattices. We can think of any planar graph \mathcal{G} as the dual object to a triangulation \mathcal{T} of the sphere or of the disk as in fig. 2, right. Each vertex configuration on \mathcal{G} determines, up to a constant, an integer-valued height function, with heights assigned to the sites of the dual triangulation \mathcal{T} . The oriented loops divide the planar graph into domains of constant heights, with the oriented loops appearing as domain boundaries. The difference of the heights on both sides of an oriented loop is ± 1 depending on the orientation. For a given loop configuration, all heights but one can be reconstructed by taking into account the loop orientations. The Boltzmann weight of a height configuration on the triangulation \mathcal{T} is a product of local factors associated with the elementary triangles Δ_{ijk} ,

$$\begin{aligned}W_{\Delta}(h_1, h_2, h_3) &= \delta_{h_1 h_2} \delta_{h_2 h_3} \delta_{h_3 h_1} + \frac{1}{T} \delta_{h_1 h_2} h_{h_2 h_3} A_{h_3 h_1} w^{h_3 - h_1} + \text{cyclic}, \\ A_{ab} &\equiv \delta_{a, b+1} + \delta_{a, b-1}.\end{aligned}\tag{3.2}$$

The partition sum in (3.1) is generated by expanding the product of the Boltzmann weights in monomials and performing the sum over the heights. Discrete models of 2D gravity based on height models on dynamical triangulations have been studied e.g. in [45].

The weights of the loops in the expansion (3.1) can be given a geometrical description in terms of the local curvature of the discretised world surface. For that we must define a metric on the elementary triangles. The simplest assumption is that the triangulated surface

is composed of flat identical equilateral triangles. The triangles can be either empty, with weight T , or contain a loop segment making right or left turn at $\pi/6$:



The phase factor for each loop in the expansion (3.1) can be thought of as a holonomy factor for a particle with spin. Each left/right turn contributes an elementary holonomy $\exp(\pm i\pi\lambda/2)$, a lattice analogue of the spin connection defined on pairs of adjacent links. The phase of the holonomy factor, a discrete analogue of the Berry phase [46], is

$$\frac{1}{2}\pi\lambda[(\text{left turns}) - (\text{right turns})] = \frac{3}{2}\lambda\hat{K}_{\mathcal{L}} \quad (3.4)$$

where $\hat{K}_{\mathcal{L}}$ is the total geodesic curvature of the oriented loop \mathcal{L} . By the Gauss-Bonnet formula, the geodesic curvature is related to the integrated Gaussian curvature $\hat{R}_{\mathcal{L}}$ inside the domain $\mathcal{T}_{\mathcal{L}}$ bounded by the loop,

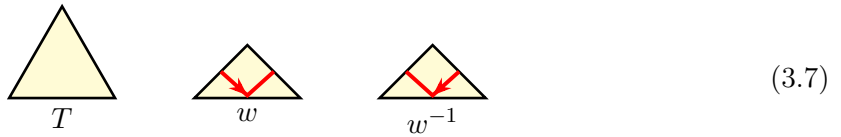
$$\hat{R}_{\mathcal{L}} + 2\hat{K}_{\mathcal{L}} = 4\pi, \quad \hat{R}_{\mathcal{L}} \equiv \sum_{i \in \mathcal{T}_{\mathcal{L}}} \hat{R}_i, \quad (3.5)$$

where the Gaussian curvature at the site $i \in \mathcal{T}$ is related in our case to the coordination number C_i by

$$\hat{R}_i = \frac{2\pi}{3}(6 - C_i). \quad (3.6)$$

For a sphere, changing the orientation of a loop exchanges the internal and the external domains and the phase factor changes sign.

This is not the only choice for the geometry of the dynamical triangulations. We can use triangles with edges of different length with the condition that only edges of the same length can be glued together. For example, we can choose the empty triangles to be equilateral with sides of unit length, assume that the triangles containing segments of loops are isosceles with one angle $\pi/2$ and two angles $\pi/4$ and long side of unit length:



Now the loop segments make turns at $\pm\pi/2$ and the phase factor of a loop \mathcal{L} is $\lambda\hat{K}_{\mathcal{L}}$. The relation (3.5) still holds, but the local curvature now is defined as

$$\hat{R}_i = 4\pi - 2 \times (\text{the total angle at the site } i). \quad (3.8)$$

Note that a flat triangulation with the choice (3.3) contains conical curvature defects with the choice (3.7) and vice versa. If $T = 0$, the triangles with the choice (3.7) can be glued

pairwise along their long sides to make squares. This brings us to the formulation of the six-vertex model on random quadrangulations [29–31].

To summarise, in the loop expansion of the gravitational 7v model, the oriented loops are weighted by a geometrical phase proportional to the geodesic curvature of the loop. The definitions of the geodesic and the Gaussian curvatures depend on the choice of the geometry of the triangular tiles the world surface is made of, but for the sum over surfaces this choice is irrelevant.

3.2 The 7-vertex matrix model

Now let us formulate the matrix model which is the holographic dual to the gravitational 7v model. The partition function of the 7v matrix model is given by the integral

$$\begin{aligned} \mathcal{Z}_N &= \int d\mathbf{X} d\mathbf{Z} d\mathbf{Z}^\dagger e^{-\frac{1}{\hbar}\mathcal{S}}, \\ \mathcal{S} &= \text{Tr} \left(\frac{1}{2}\mathbf{X}^2 + \mathbf{Z}\mathbf{Z}^\dagger - \frac{T}{3}\mathbf{X}^3 - w\mathbf{X}\mathbf{Z}\mathbf{Z}^\dagger - w^{-1}\mathbf{X}\mathbf{Z}^\dagger\mathbf{Z} \right). \end{aligned} \quad (3.9)$$

The integration variables \mathbf{X} and \mathbf{Z} are respectively Hermitian and complex $N \times N$ matrices with flat integration measure

$$d\mathbf{X} d\mathbf{Z} d\mathbf{Z}^\dagger = \prod_{i,j} dX_{ij} dZ_{ij} d\bar{Z}_{ij}. \quad (3.10)$$

The perturbative free energy of the 7v matrix model is a sum over all connected planar (i.e. with thickened lines) Feynman graphs with vertices as in fig. 1. The topology of the planar graphs is controlled by the Planck constant $\hbar \sim 1/N$, and the asymptotic semiclassical expansion of the free energy of the matrix model is also a topological expansion,

$$\hbar^2 \log \mathcal{Z}_N = \sum_{g \geq 0} \hbar^{2g} \mathcal{F}_g(\kappa, \lambda), \quad \kappa = \hbar N, \quad (3.11)$$

with $\mathcal{F}_g(\kappa, \lambda)$ being the contribution of the planar graphs with g handles.

The gaussian integral over the complex matrix can be done explicitly, leaving an integral over the hermitian matrix \mathbf{X} which, after factoring out the volume of the $\mathbf{SU}(N)$ group, reduces to an N -fold integral with respect to the real eigenvalues x_1, \dots, x_N ,

$$\mathcal{Z}_N \sim \int \prod_{j=1}^N dx_j e^{-\frac{1}{\hbar}(\frac{1}{2}x_j^2 - \frac{T}{3}x_j^3)} \prod_{k \neq j} \frac{x_k - x_j}{1 - wx_k - w^{-1}x_j}. \quad (3.12)$$

Strictly speaking, the integral is divergent because the cubic potential is not bounded from below. In addition, the integrand has a simple pole at

$$x_i = 1/r, \quad r = 2 \cos(\pi\lambda/2) > 0 \quad (i = 1, \dots, N). \quad (3.13)$$

However, if we are interested only in the large N expansion, we can ignore these divergencies. With the assumption $\lambda \in [0, 1]$, for $T > 0$ the position of the pole is between the minimum at $x = 0$ and the maximum at $x = T$ of the external cubic potential. If the pole is

outside of the equilibrium distribution of the eigenvalues around the minimum we can, up to exponentially small corrections, restrict the integration to $x < 1/r$. After a linear change of the variable sending the pole to the origin, the eigenvalue integral takes the form, up to a normalisation,

$$\mathcal{Z}_N \sim \int_{-\infty}^0 \prod_{j=1}^N dx_j e^{-\frac{1}{\hbar}V(x_j)} \frac{\prod_{k < j} (x_k - x_j)^2}{\prod_{k,j} (q^{1/2}x_k - q^{-1/2}x_j)}, \quad q = e^{i\pi(1+\lambda)}, \quad (3.14)$$

where $V(x)$ is a cubic potential. For $T = 0$, this is the eigenvalue integral for the 6v matrix model [29].³

In view of the comparison with the MQM approach to sine-Liouville gravity [13], we will consider the grand canonical ensemble

$$\mathcal{Z}(\tilde{\kappa}) = \sum_{N=1}^{\infty} e^{-N\tilde{\kappa}/\hbar} \mathcal{Z}_N \quad (3.15)$$

where the chemical potential $\tilde{\kappa}$ plays the role of the lattice cosmological constant. The grand partition function is a Fredholm determinant

$$\mathcal{Z}(\tilde{\kappa}) = \det(1 + K), \quad (3.16)$$

with the Fredholm kernel

$$K(x, x') \equiv \frac{e^{-\frac{\tilde{\kappa}+V(x)}{i\hbar}}}{q^{-1/2}x - q^{1/2}x'}, \quad (3.17)$$

defined with flat integration measure dx on the negative axis.

To compute the genus-zero free energy \mathcal{F}_0 which is the sphere partition function of the gravitational 7v model, we take the thermodynamical limit $\hbar \rightarrow 0, N \rightarrow \infty$ with $\kappa = N\hbar$ fixed. Then the sum in (3.15) is saturated by the saddle-point

$$\partial_{\kappa}\mathcal{F}_0(\kappa) = \tilde{\kappa}, \quad \mathcal{F}_0(\kappa) = \hbar^2 \log \mathcal{Z}_{\kappa/\hbar}. \quad (3.18)$$

The grand free energy $\mathcal{F}(\tilde{\kappa}) = \hbar^2 \log \mathcal{Z}(\tilde{\kappa})$ is related to the canonical one by Legendre transformation

$$\tilde{\mathcal{F}}_0(\tilde{\kappa}) = -\tilde{\kappa}\kappa + \mathcal{F}_0(\kappa). \quad (3.19)$$

The basic observable, which serves as a building block for most of the observables, is the L -th moment of the matrix \mathbf{X} ,

$$W_L = \hbar \langle \text{Tr}(\mathbf{X}^L) \rangle, \quad (3.20)$$

³Integrals of this type have appeared previously in different contexts: relativistic membranes [47], dimensional reduction of SYM [48, 49], Euclidean black hole [12], Leigh-Strassler deformations of supersymmetric gauge theories [50, 51], and more recently, with non-polynomial potential, as matrix models for topological strings on Calabi-Yau threefolds [52, 53]. Combinatorial aspects of the planar graph expansion of the model (3.9) were addressed in [54].

where the expectation value of the trace in the grand ensemble (3.15) is defined as the sum, with a weight $e^{-\tilde{\kappa}N/\hbar}$, of the unnormalised expectation values in the sectors with N eigenvalues. The resolvent of the random matrix

$$W(x) = \sum_{L=0}^{\infty} x^{-L-1} W_L = \hbar \left\langle \text{Tr} \frac{1}{x - \mathbf{X}} \right\rangle \quad (3.21)$$

represents the disk amplitude $W(x)$ with marked boundary and (complexified) boundary cosmological constant x .

3.3 Collective field and Virasoro constraint

The grand partition function (3.15) has the form of a Coulomb gas and can be formulated in terms of a collective bosonic field with mode expansion

$$\varphi(x) = \varphi_0 + \alpha_0 \log x - \sum_{n \neq 0} \frac{x^{-n}}{n} \alpha_n, \quad [\alpha_n, \alpha_m] = n \delta_{m+n,0}, \quad [\varphi_0, \alpha_0] = 1. \quad (3.22)$$

The Hilbert space is built on the Fock vacua defined by

$$\langle 0 | \alpha_n = 0 \quad (n \leq 1), \quad \alpha_0 | 0 \rangle = 0 \quad (n \geq 1), \quad \langle 0 | \varphi_0 = \alpha_0 | 0 \rangle = 0, \quad (3.23)$$

and the two-point function is

$$\langle 0 | \varphi(x) \varphi(x') | 0 \rangle = \log(x - x'). \quad (3.24)$$

To generate the pairwise interaction of the eigenvalues, which is that of dipoles composed of a positive charge at $q^{1/2}x_j$ and a negative charge at $q^{-1/2}x_j$, we must introduce two more bosonic fields, $\mathbf{S}(x)$ and $\varphi(x)$, related to the principal field $\varphi(x)$ as

$$\begin{aligned} \mathbf{S}(x) &= \frac{\varphi(q^{1/2}x) - \varphi(q^{-1/2}x)}{i} \\ \varphi(x) &= \alpha_0 \log x + \frac{\Omega(q^{1/2}x) - \Omega(q^{-1/2}x)}{i}. \end{aligned} \quad (3.25)$$

The mode expansion of the two auxiliary fields is, with $\beta = \pi(1 + \lambda)$,

$$\begin{aligned} \mathbf{S}(x) &= \beta \alpha_0 - \sum_{n \neq 0} 2 \sin(\tfrac{1}{2}n\beta) \frac{x^{-n}}{n} \alpha_n, \\ \Omega(x) &= \frac{1}{\beta} \varphi_0 \log x - \sum_{n \neq 0} \frac{1}{2 \sin(\tfrac{1}{2}n\beta)} \frac{x^{-n}}{n} \alpha_n. \end{aligned} \quad (3.26)$$

the correlation function of these two fields is

$$\langle 0 | \Omega(x) \mathbf{S}(x') | 0 \rangle = \log(x - x'). \quad (3.27)$$

The field $\mathbf{S}(x)$ generates the Coulomb interaction of the eigenvalues and the dual field $\Omega(x)$ generates the external potential. With the help of these two fields, we express the grand partition function (3.15) as a Fock space expectation value

$$\mathcal{Z}(\tilde{\kappa}) = \langle 0 | \mathbf{U}_- \mathbf{U}_+ | 0 \rangle \quad (3.28)$$

of the product of the exponential operators

$$\begin{aligned}\mathbf{U}_- &= \exp \left[-\frac{1}{\hbar} \left(\oint_{\infty} (\tilde{\kappa} + V(x)) \frac{d\mathbf{\Omega}(x)}{2\pi i} \right) \right], \\ \mathbf{U}_+ &= \exp \left[\int_{\mathbb{R}} dx : e^{-\mathbf{S}(x)} : \right],\end{aligned}\tag{3.29}$$

with the normal ordering defined so that the operators α_n with $n \geq 0$ are on the right. The partition function is generated by expanding the exponential in the second factor and applying the operator product expansions

$$\begin{aligned}\mathbf{\Omega}(x) : e^{-\mathbf{S}(x')} : &\sim \log(x - x') : e^{-\mathbf{S}(x')} : \\ : e^{-\mathbf{S}(x)} : : e^{-\mathbf{S}(x')} : &\sim \frac{(x - x')^2}{(x - q^{-1}x')(x - qx')} : e^{-\mathbf{S}(x)} e^{-\mathbf{S}(x')} :, \end{aligned}\tag{3.30}$$

With the expectation value of the operator \mathbf{O} defined as

$$\langle \mathbf{O} \rangle = \mathcal{Z}(\tilde{\kappa})^{-1} \langle 0 | \mathbf{U}_- \mathbf{O} \mathbf{U}_+ | 0 \rangle,\tag{3.31}$$

the oscillators φ_0 and α_0 represent $\tilde{\kappa}$ and $\partial/\partial\tilde{\kappa}$:

$$\tilde{\kappa} = \beta\hbar \langle \alpha_0 \rangle, \quad \frac{\partial \mathcal{F}(\tilde{\kappa})}{\partial \tilde{\kappa}} = -\frac{\hbar}{\beta} \langle \varphi_0 \rangle.\tag{3.32}$$

where $\mathcal{F}(\tilde{\kappa}) = \hbar^2 \log \mathcal{Z}(\tilde{\kappa})$ is the all-genus free energy of the matrix model.

We normalise the expectation values so that in the limit $\hbar \rightarrow 0$ they remain finite: $S(x) \equiv \hbar \langle \mathbf{S}(x) \rangle$, etc. The expectation value of $\mathbf{S}(x)$ consists of a polynomial piece, $S_{\infty}(x) = V(x) + \tilde{\kappa}$, and a piece regular at infinity:

$$S(x) \equiv \hbar \langle \mathbf{S}(x) \rangle = S_{\infty}(x) + O(1/x), \quad S_{\infty}(x) = V(x) + \tilde{\kappa}.\tag{3.33}$$

Similarly for φ and $\mathbf{\Omega}$, with φ_{∞} and Ω_{∞} determined by the defining relations (3.25), and for the currents

$$\mathbf{H}(x) = \partial \mathbf{S}(x), \quad \mathbf{Y}(x) = \partial \varphi(x), \quad \mathbf{J}(x) = \partial \mathbf{\Omega}(x).\tag{3.34}$$

The basic observable (3.21) is given by the regular at infinity piece of the expectation value of the current $\mathbf{J}(x)$:

$$W(x) = \hbar \langle \mathbf{J}(x) \rangle - J_{\infty}(x).\tag{3.35}$$

The observables in the matrix model can be obtained with the help of a conformal Ward identity for the collective field, often referred to as the Virasoro constraint, which follows from the OPE

$$: \mathbf{H}(x)^2 : : e^{-\mathbf{S}(x')} : \sim \partial_{x'} \left(\frac{1}{x - x'} : e^{-\mathbf{S}(x')} : \right) + \text{regular}.\tag{3.36}$$

The total derivative form of the rhs insures that the operator $:\mathbf{H}^2(x):$ commutes, up to exponentially vanishing boundary terms, with the operator \mathbf{U}_+ in (3.28). Hence for any operator \mathbf{O}

$$\oint_c \frac{dx'}{x-x'} \langle \mathbf{O} : \mathbf{H}(x')^2 : \rangle = 0, \quad (3.37)$$

where the integration contour encloses the real axis and leaves outside all other singularities of the integrand, including the point x . The Virasoro constraint (3.37) is equivalent to the statement that the integrand is analytic in the vicinity of the real axis. The conformal Ward identity (3.37) can also be formulated in terms of the current $\mathbf{Y}(x)$, as the statement that for any operator \mathbf{O} ,

$$\langle \mathbf{O} \cdot \mathbf{Y}(q^{1/2}x) \mathbf{Y}(q^{-1/2}x) \rangle \text{ is analytic in the vicinity of the real axis.} \quad (3.38)$$

Of course, the Virasoro constraint can also be derived directly for the matrix integral as a Dyson-Schwinger equation reflecting translation invariance of the measure. The Ward identities (3.37) or (3.38) can be used to reconstruct the whole genus expansion of the free energy. Here we are focusing on the observables on the disk and on the sphere and will take the semiclassical limit $\hbar \rightarrow 0$ where the expectation values of traces factorise and the Virasoro constraint becomes a quadratic functional equation for a c -function.

4 Thermodynamical limit and spectral curve

4.1 Boundary value problem

In the limit $\hbar \rightarrow 0$, the fluctuations of the collective field are suppressed and the basic observables are determined completely by the saddle-point spectral density $\rho(x)$ or, equivalently, by the resolvent

$$W(x) = \hbar \left\langle \text{Tr} \frac{1}{x - \mathbf{X}} \right\rangle = \int_{\mathbb{R}} \frac{dx' \rho(x')}{x - x'} \quad (4.1)$$

which by definition is analytic in the x -plane with a cut on some interval $[-a, -b]$ with $a > b > 0$. The expectation values of the three currents,

$$\begin{aligned} J(x) &= \partial\Omega(x) = W(x) + J_\infty(x), \\ Y(x) &= \partial\varphi(x) = \frac{q^{1/2}W(q^{1/2}x) - q^{-1/2}W(q^{-1/2}x)}{i} + Y_\infty(x), \\ H(x) &= \partial S(x) = 2W(x) - qW(qx) - q^{-1}W(q^{-1}x) + H_\infty(x), \end{aligned} \quad (4.2)$$

have respectively one, two and three cuts on rays obtained by rotating the real axis.

As the resolvent $W(x)$ itself does not have simple form even in the continuum limit, it is more convenient to formulate the observables in terms of the function $y = Y(x)$ which will be the classical spectral curve for our problem. The spectral curve is determined uniquely

its asymptotics at infinity together with the classical Virasoro constraint (3.38), which is equivalent to the boundary value problem

$$q^{1/2}Y(q^{1/2}e^{\mp i\epsilon}x) = q^{-1/2}Y(q^{-1/2}e^{\pm i\epsilon}x), \quad x \in [-a, -b]. \quad (4.3)$$

This condition for $Y(x)$ is equivalent to $S(x)$ being constant on the interval $[-a, -b]$. By the second equation (3.32), the constant is equal to $\tilde{\kappa}$.

Once the function $Y(x)$ is known, the classical resolvent $W(x)$ is completely determined by the relations (4.2). To express the spectral density in terms of $Y(x)$, we write the second relation (4.2) as

$$W(x) = iq^{1/2}Y(q^{1/2}x) + e^{i\beta}W(qx) + \text{polynomial in } x. \quad (4.4)$$

Since $W(x)$ is, by definition, a real analytic function, only the first term in the r.h.s. has a cut $[-a, -b] \subset \mathbb{R}$. The discontinuity of $W(x)$ across this cut is therefore that of the first term, and equal to twice its imaginary part,

$$\rho(x) \equiv \frac{1}{\pi} \Im W(x) = \frac{1}{\pi} \Re \left[q^{1/2}Y(q^{1/2}) \right] \quad \text{for } x \in [-a, -b]. \quad (4.5)$$

The spectral curve of our problem defines an infinitely foliated Riemann surface. By introducing an elliptic uniformisation map to resolve the four branch points, eq. (4.3) can be transformed into periodicity along the A -cycle and quasi-periodicity along the B -cycle of the parametrisation torus. In the x -plane, the A -cycle is represented by a closed contour enclosing the upper cut while the B -cycle is represented by an open contour \mathcal{C}_B connecting the upper edge of the lower cut to the lower edge of the upper cut. Then we can write eq. (3.32) in the thermodynamical limit as

$$\tilde{\kappa} = \frac{1}{i} \int_{\mathcal{C}_B} Y dx, \quad \partial_{\tilde{\kappa}} \mathcal{F}_0 = -\frac{1}{2\pi} \oint_{\mathcal{C}_A} Y dx. \quad (4.6)$$

4.2 Phase diagram and scaling limit

The gravitational 7v model is a deformation of the gravitational $O(2)$ loop model and should have qualitatively the same phase diagram characterised by dense, dilute and massive phases of the loop gas. To describe the critical phases let us return to the canonical ensemble (fixed κ) where the phase diagram is drawn in the (κ, T) -plane.

When κ increases with T fixed, at some critical value $\kappa = \kappa_c(T)$ the partition sum diverges because of the volume of the planar graphs. This is the phase of pure gravity. On the other hand, if we keep κ constant and decrease the temperature, below some $T = T_c(\kappa)$ the effective tension of the loops will become negative and the planar graph will be densely filled with loops. This is the critical phase of dense loops with effective bare cosmological constant $\kappa_1 = \kappa/T$. The two critical lines join at the tricritical point (κ_*, T_*) where the length of the loops diverges but the volume not occupied by loops also diverges. At this point a third critical phase emerges, the phase of dilute loops.

In the grand ensemble, the critical point is at $(\tilde{\kappa}_*, T_*)$ with $\tilde{\kappa}_*$ related to κ_* by (3.18). The continuum limit concerns the blown-up vicinity of the tricritical point in the double scaling limit parametrised by the renormalised coupling constants

$$x \rightarrow \epsilon x, \quad \tilde{\kappa}_* - \tilde{\kappa} \rightarrow \epsilon^{2/(1-\lambda)} 2\pi\mu, \quad T - T_* \rightarrow \epsilon^{4\lambda/(1-\lambda^2)} t, \quad (4.7)$$

where ϵ is a small elementary length and where we anticipated the critical indices obtained from the analytic solution we are going to derive below. The properly normalised observables in the limit $\epsilon \rightarrow 0$ will be given by scaling functions of the dimensionless combinations $\hat{t} \sim t/\mu^{2\lambda/(1+\lambda)}$ and $\hat{x} \sim x/\mu^{(1-\lambda)/2}$. The dense critical phase is achieved at $t \rightarrow -\infty$ and is characterised by another set of exponents.

4.3 Uniformisation of the boundary value problem in the scaling limit

The exact solution of the boundary value problem will be reported in a future publication [34]. Here we focus on the continuum limit when the parametrisation torus degenerates into a cylinder, with the large cycle defining a UV cutoff.

The scaling limit is achieved by taking $\epsilon \sim b/a \rightarrow 0$ and simultaneously rescaling x so that the right branch point stays at a finite distance M_b from the origin while the left branch point escapes to $-\infty$. From now on, x denotes the rescaled variable x . The analytic properties of the function $y = Y(x)$ change accordingly. In the scaling limit, the Riemann surface of $Y(x)$ has two semi-infinite cuts in the main sheet starting at $q^{\pm 1}M_b$ and ending at infinity in the lower/upper semi-plane x (fig. 3, left). Such analytic structure results in two distinct points at infinity, $\Re x \rightarrow +\infty$ and $\Re x \rightarrow -\infty$. One can imagine the Riemann surface as an infinite cover of a sphere with singularities at the north and at the south poles. At the two singular points, the function $Y(x)$ has two different expansions in fractional powers of $1/x$, convergent respectively in the domains \mathbb{C}_+ and \mathbb{C}_- delimited by the two cuts and presented in fig. 3 in yellow and green.

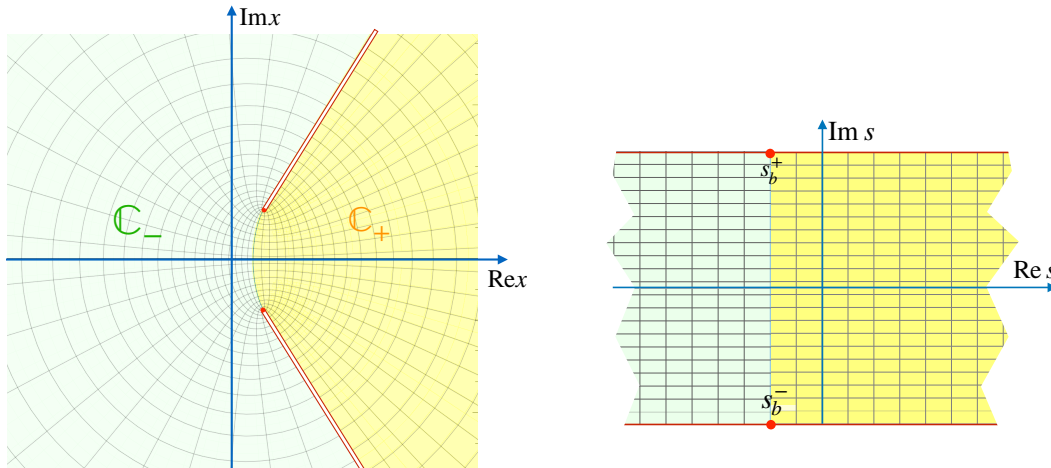


Figure 3. The domains \mathbb{C}_+ and \mathbb{C}_- of the principal sheet of the Riemann surface of $Y(x)$ (left) and in the principal strip of the s -parametrisation plane (right)

The two cuts are resolved by a uniformisation map $s \rightarrow x$ such that the main sheet of the Riemann surface of $Y(x)$ is parametrised by a strip of width π in the s -plane (fig. 3, right)

$$x(s) = 2M e^{-\lambda s} \sinh s, \quad s \in \mathbb{R} \times \left[-\frac{1}{2}i\pi, \frac{1}{2}i\pi\right]. \quad (4.8)$$

The whole Riemann surface is parametrised by extending the map (4.8) to $s \in \mathbb{C}$. The upper and the lower cut are the images of the upper and the lower edge of the parametrisation strip and the pre-images of the two singular points are at $\Re s \rightarrow \pm\infty$.

The parameter M determines the positions of the branch points where $x'(s) = 0$. Besides the two simple branch points in the main sheet, there is an infinite number of simple branch points in the lower sheets whose parameters form a vertical array $s_b + 2\pi i(n + 1/2)$ with $n \in \mathbb{Z}$ and

$$s_b = \log b < 0 \quad (b^2 = \frac{1-\lambda}{1+\lambda}). \quad (4.9)$$

The two branch points x_b^\pm in the first sheet are

$$x_b^\pm = x(s_b \pm i\pi/2) = -q^{\pm 1/2} M_b, \quad (4.10)$$

with

$$M_b = (1 + b^{-2}) b^{\frac{2}{1+b^2}} M. \quad (4.11)$$

The domain \mathbb{C}_+ is parametrised by the semi-infinite strip $|\Im s| < \pi/2$, $\Re s > s_b$ and the complementary domain \mathbb{C}_- is parametrised by the half-strip $|\Im s| < \pi/2$, $\Re s < s_b$, as depicted in fig. 3, right.

The uniformisation map (4.8) transforms the boundary value problem into a monodromy problem. The sewing condition (4.3) for $Y(x)$ can be formulated as a quasi-periodicity condition for the functions $x(s)$ and $y(s) = Y[x(s)]$,

$$\begin{aligned} x(s \pm i\pi/2) &= e^{\pm i\beta} x(s \mp i\pi/2), \\ y(s \pm i\pi/2) &= e^{\mp i\beta} y(s \mp i\pi/2). \end{aligned} \quad (4.12)$$

The quasiperiodicity condition (4.12) has infinitely many solutions classified by their asymptotics at infinity. The correct asymptotics is determined by the external potential but after taking the scaling limit we do not have access to this information. In order to be able to recognise the solution relevant for our problem, let us first consider the critical point where $M_b \rightarrow 0$.

4.4 Solution at the critical point ($M = 0$)

At the critical point, the bridge connecting the two domains \mathbb{C}_+ and \mathbb{C}_- disappears and the solution must be sought separately in each of them,

$$\begin{aligned} \mathbb{C}_- : \quad Y(e^{i\beta} x) &= e^{-i\beta} Y(x) & \Rightarrow \quad Y(x) &\sim (-x)^{\frac{2n}{1+\lambda}-1}, \\ \mathbb{C}_+ : \quad Y(e^{i(2\pi-\beta)} x) &= e^{-i(2\pi-\beta)} Y(x) & \Rightarrow \quad Y(x) &\sim x^{\frac{2n}{1-\lambda}-1}. \end{aligned} \quad (4.13)$$

The integer n should be positive because the density must vanish at the origin. The most general solution for the resolvent is therefore

$$W(x) = \sum_{n \geq 1} t_n^+ \frac{x^{\frac{2n}{1-\lambda}-1}}{2 \sin(\pi n/b^2)} - \sum_{n \geq 1} t_n^- \frac{(-x)^{\frac{2n}{1+\lambda}-1}}{2 \sin(\pi n b^2)}. \quad (4.14)$$

Indeed, from the second relation (4.2) we obtain

$$Y(x) = \begin{cases} -\sum_{n \geq 1} t_n^- (-x)^{\frac{2n}{1+\lambda}-1} & \text{if } x \in \mathbb{C}_-, \\ \sum_{n \geq 1} t_n^+ x^{\frac{2n}{1-\lambda}-1} & \text{if } x \in \mathbb{C}_+. \end{cases} \quad (4.15)$$

In the case of a cubic potential before the scaling limit, the solution must be a combination of the lowest powers in each of the domains,

$$Y(x) = \begin{cases} -t (-x)^{\frac{1-\lambda}{1+\lambda}} & \text{if } x \in \mathbb{C}_-, \\ x^{\frac{1+\lambda}{1-\lambda}} & \text{if } x \in \mathbb{C}_+, \end{cases} \quad (4.16)$$

where we rescaled x to have $t_1^+ = 1$, $t_1^- = t$. Scaling solutions of more general form can be obtained by starting with polynomial potential of higher degree and tuning the coefficients.

Taking the discontinuity of the resolvent, one finds for the critical spectral density

$$\rho(x) = \frac{|x|^{\frac{1}{b^2}} + t|x|^{b^2}}{2\pi}, \quad x < 0, \quad (4.17)$$

with b defined by (1.4). The rhs of (4.16) determines the large- x asymptotics of the solution in the continuum limit we are looking for.

4.5 Solution of the boundary value problem in the continuum limit

The unique solution of the quasi-periodicity condition (4.12) with asymptotics (4.16) at $|x| \rightarrow \infty$ is

$$\begin{aligned} x(s) &= 2M e^{-\lambda s} \sinh s, \\ y(s) &= e^{(1+\lambda)s} M^{\frac{1+\lambda}{1-\lambda}} - t e^{-(1-\lambda)s} M^{\frac{1-\lambda}{1+\lambda}}. \end{aligned} \quad (4.18)$$

This solution corresponds to a certain normalisation of the coupling constants μ and t in the scaling limit (4.7).

With a change of the parameter $s \rightarrow \omega = e^{-2s/(b+b^{-1})}$, this solution takes the form (1.5) announced in the Introduction. The function $y = Y(x)$ is determined in the domains \mathbb{C}_\pm by two different power series whose positive parts are given in our case by (4.15).

The spectral curve in the continuum limit matching the general solution (4.16) has the parametric form

$$\begin{aligned} x(s) &= M e^{(1-\lambda)s} - M^{-(1+\lambda)s}, \\ y(s) &= \sum_{n \geq 1} \left(t_n^+ M^{\frac{2n}{1-\lambda}-1} e^{(2n+\lambda)s} - t_n^- M^{\frac{2n}{1+\lambda}-1} e^{-(2n-\lambda)s} \right). \end{aligned} \quad (4.19)$$

For a finite number of non-vanishing couplings, this solution describes the vicinity of a multicritical point of a more general vertex model, in close analogy with the $O(2)$ model analysed in [32]. For example, the tricritical point represents microscopically the vertex model in the presence of vacancies and dimers with negative fugacity.

The fact that the solution has different asymptotics at $x \rightarrow +\infty$ and $x \rightarrow -\infty$ marks an important difference between the gravitational vertex model and the other solved models

of 2D QG. In the $O(2)$ model, which corresponds to $\lambda = 0$, the uniformisation map has the symmetry $s \rightarrow -s$. Because of this symmetry the parameters of the branch points must be at $s_{\text{b}}^{\pm} = \pm i\pi/2$ and the two infinite-order branch points at $\Re s \rightarrow \pm\infty$ can be identified. This \mathbb{Z}_2 symmetry is present also in the $O(n)$ model with $|n| < 2$ and in all generalised minimal models of 2D gravity, but not in the vertex models.

4.6 Computation of the boundary entropy

The parameter $M = M(\mu, t)$ is related to the position $x = -M_{\text{b}}$ of the edge of the eigenvalue distribution. This is the critical value of the boundary cosmological constant and can be interpreted as the renormalised boundary entropy of the sine-Liouville gravity on a disk.

To determine the function $M = M(\mu, t)$, we substitute the solution (4.18) in equations (4.6). We write these equations in terms of the function

$$\varphi(s) = \int^s y(s') dx(s') = c_+ e^{2s} + c_- e^{-2s} + c_3 s + \text{const} \quad (4.20)$$

with

$$c_{\pm} = \frac{1}{2}(1 \mp \lambda) M^{\frac{2}{1 \mp \lambda}} \quad \text{and} \quad c_3 = (1 + \lambda) M^{\frac{2}{1 - \lambda}} - (1 - \lambda) t M^{\frac{2}{1 + \lambda}}. \quad (4.21)$$

In the parametrisation strip, the now infinite A -cycle connects the points $s = -\infty$ with $s = +\infty$, and the B -cycle connects the two edges of the s -parametrisation strip. The second relation (4.6) states, in terms of $\varphi(s) \equiv \varphi[x(s)]$, that for any s ,

$$S(s) \equiv \frac{\varphi(s + i\pi/2) - \varphi(s - i\pi/2)}{i} = 2\pi\mu. \quad (4.22)$$

Only the last term in (4.20) contributes to the difference and we arrive at the transcendental (for irrational λ) equation (1.6) for the boundary entropy $M = M(\mu, t)$,

$$\mu = \frac{1 + \lambda}{2} M^{\frac{2}{1 - \lambda}} - \frac{1 - \lambda}{2} t M^{\frac{2}{1 + \lambda}}. \quad (4.23)$$

This equation implies the scaling law we anticipated in (4.7). The function $M(\mu, t)$ is obtained as a power series

$$M = -\frac{1 - \lambda}{2} \left(\frac{2\mu}{1 + \lambda} \right)^{\frac{1 - \lambda}{2}} \sum_{n=0}^{\infty} \frac{\Gamma\left(n\lambda(1 - b^2) - \frac{b^2}{1 + b^2}\right)}{\Gamma\left(\frac{1}{1 + b^2} - nb^2\right)} \frac{(-\hat{t})^n}{n!} \quad (4.24)$$

where \hat{t} denotes the dimensionless coupling

$$\hat{t} \equiv b^2 (2\mu)^{-\frac{2\lambda}{1 + \lambda}} t. \quad (4.25)$$

4.7 Partition function on the sphere and susceptibility

Now we will find the derivative of the partition function on the sphere from the first equation (4.6). The contour integral of $Y dx = d\varphi(x)$ becomes, in the s -parametrisation, the linear integral along one of the two boundaries of the parametrisation strip,

$$\partial_{\mu} \mathcal{F}_0 = - \int_{\Im s = \pi/2} y(s) dx(s). \quad (4.26)$$

It is easier to derive an equation for the second derivative $u = \partial_\mu^2 \mathcal{F}$ often called the susceptibility. Let us first compute the derivative $\partial_\mu Y(x)$ using the s -parametrisation,

$$\partial_\mu Y(x) \equiv \partial_\mu y(s)|_x = \partial_\mu M \left(\frac{\partial y(s)}{\partial M} \Big|_s - \frac{\partial x(s)}{\partial M} \Big|_s \frac{y'(s)}{x'(s)} \right) = \frac{2}{x'(s)}. \quad (4.27)$$

This relation is in fact quite general and reflects the existence of a classical one-dimensional Hamiltonian system for which $x = x(s), y = y(s)$ define a classical phase-space trajectory, with $\varphi(s)$ being the abbreviated action. Since $\partial_\mu x = 0$, eq. (4.27) can be written in the form of Poisson bracket,

$$\{x, y\} = 2, \quad \text{with} \quad \{f, g\} \equiv \frac{\partial f}{\partial s} \frac{dg}{\partial \mu} - \frac{\partial g}{\partial s} \frac{df}{\partial \mu}. \quad (4.28)$$

Now we can obtain the derivative $\partial_\mu \varphi$ by integrating both sides of (4.27),

$$\partial_\mu \varphi(s)|_x = \int \partial_\mu [y(s)x'(s)]_x ds = \int \partial_\mu y(s)|_x x'(s) ds = 2s. \quad (4.29)$$

Since the A -cycle becomes infinite in the continuum limit, we regularise the integral (4.26) by introducing an UV cutoff Λ . Retaining only the leading term in the large x expansion, we have

$$u \equiv \partial_\mu^2 \mathcal{F}_0 = -(\partial_\mu \varphi|_{x=\Lambda} - \partial_\mu \varphi|_{x=-\Lambda}) \approx -\frac{4}{1-\lambda^2} \log \frac{\Lambda}{M}. \quad (4.30)$$

Now we can substitute in (4.23)

$$M = e^{-\frac{1-\lambda^2}{4}u}. \quad (4.31)$$

from (4.30) to arrive at equation (1.7) for the susceptibility,

$$\mu = \frac{1+\lambda}{2} e^{-\frac{1+\lambda}{2}u} - \frac{1-\lambda}{2} t e^{-\frac{1-\lambda}{2}u}. \quad (4.32)$$

The three critical points of this equation correspond to the expected three scaling regimes of the sine-Liouville gravity, $t = 0$, $t \rightarrow -\infty$ and $t = t_c > 0$. The third critical point is determined by $\partial\mu/\partial M|_{t=t_c} = 0$. In the vicinity of the three critical points, the free energy is given by

$$\mathcal{F}_0 = \begin{cases} -\frac{1}{1+\lambda} \mu^2 \log \frac{2\mu}{1-\lambda} & (t \rightarrow 0), \\ -\frac{1}{1-\lambda} \mu^2 \log \frac{2\mu}{(1-\lambda)t} & (t \rightarrow -\infty) \\ -\text{const} \times (t_c - t)^{5/2} & (t \rightarrow t_c - 0). \end{cases} \quad (4.33)$$

Since μ_B scales as M , eq. (4.23) gives different scaling of the boundary length with the area both in the dense and in the dilute phases. In the dilute critical phase $\ell \sim A^{\frac{1-\lambda}{2}}$ and in the dense phase $\ell \sim A^{\frac{1+\lambda}{2}}$. Both scalings are anomalous for $\lambda > 0$ ($b < 1$) in contrast to the gravitational $O(n)$ model, where only the scaling in the dense phase is anomalous.

4.8 UV and IR compactification radii

Here we give arguments for the relation (2.12) between the compactification circles at $t = 0$ and $t \rightarrow -\infty$.

In the dense critical phase $t \rightarrow -\infty$, where the scaling limit is that of the 6-vertex model coupled to gravity, the comparison with the Matrix Quantum Mechanics gives for the compactification radius

$$R_{\text{IR}}^{\text{SL}} = \frac{1 - \lambda}{2}. \quad (4.34)$$

On the other hand, the scaling law we obtained in the dilute critical phase $t = 0$, eq. (4.7), matches the scaling (2.11) in the UV limit of the sine-Liouville theory if

$$2 - \frac{1}{R} = \frac{2\lambda}{1 + \lambda} \quad \Rightarrow \quad R_{\text{UV}}^{\text{SL}} = \frac{1 + \lambda}{2}. \quad (4.35)$$

Eq. (2.12) follows. Comparing (4.35) with (2.9) and (2.14), we can identify

$$p = \frac{1}{\lambda}. \quad (4.36)$$

Let us conclude with two observations. First, the equation of state (4.32) has been derived previously in [12] in the context of MQM perturbed by a condensate of winding modes and its small t expansion reproduces the correlation functions of the sine-Liouville perturbation conjectured by Moore [1]. The large t expansions is then automatically obtained using the symmetry of the equation under

$$\mu \rightarrow \mu_1 = -\frac{\mu}{t}, \quad \lambda \rightarrow -\lambda, \quad t \rightarrow -1/t. \quad (4.37)$$

The symmetry of the equation is compatible with the phase structure of the sine-Gordon model and with the expressions (4.34) and (4.35) being related by $\lambda \rightarrow -\lambda$.

Second, the expressions for the free energy in (4.33) are proportional to the T-dual compactification radii. This means that the concerning the free energy, the continuum limit of the gas of oriented loops describes the fluctuations of the T-dual field $\tilde{\varphi}$.

4.9 Boundary length distribution

In the scaling limit, the disk partition functions for fixed boundary constant x and for fixed boundary length ℓ are related by Laplace transformation,

$$W(x) = \int_0^\infty d\ell \tilde{W}(\ell) e^{-\ell x}, \quad \tilde{W}_\ell = \frac{1}{2\pi i} \int_{\uparrow} dx e^{\ell x} W(x), \quad (4.38)$$

where in the last integral the contour goes in the imaginary direction, to the right of the branch points. We cannot express the resolvent in a closed form, but from the second relation (4.2) which reads, for the inverse Laplace images,

$$\tilde{Y}(\ell) = \frac{1}{i} \left(\tilde{W}(q^{1/2}\ell) - \tilde{W}(q^{-1/2}\ell) \right), \quad (4.39)$$

we can reconstruct the small ℓ expansion of $\tilde{W}(\ell)$ from the inverse Laplace image of $Y(x)$. The integral can be expressed as a difference of two linear integrals by closing the contour around the two cuts of $Y(x)$. After partial integration,

$$\tilde{Y}(\ell) = \frac{1}{2\pi i} \int_{\uparrow} dx Y(x) e^{\ell x} = -\frac{1}{\ell} \Im \int_{-\infty}^{\infty} e^{\ell x(s+i\pi/2)} dy(s+i\pi/2). \quad (4.40)$$

Then $\tilde{W}(\ell)$ is reconstructed from (4.39) with the help of (4.12),

$$\tilde{W}(\ell) = \frac{1}{\ell} \int_{-\infty}^{\infty} e^{-\ell M(e^{-(1+\lambda)s} + e^{(1-\lambda)s})} d\left(M^{\frac{1+\lambda}{1-\lambda}} e^{-(1+\lambda)s} + tM^{\frac{1-\lambda}{1+\lambda}} e^{(1-\lambda)s}\right). \quad (4.41)$$

The integral (4.40) can be expressed in terms of a generalised Bessel integral known as the Krätzel function [36] (see also e.g. [55, 56]) which we denote by $K_{\nu}^{(b)}(z)$ so that for $b = 1$ it coincides with the Bessel-K function,

$$K_{\nu}^{(b)}(2z) = \frac{1}{2} \int_0^{\infty} e^{-z(\omega^{1/b} + \omega^{-b})} \omega^{\nu-1} d\omega, \quad \Re z > 0. \quad (4.42)$$

The function $K_{\nu}^{(b)}(z) = K_{-\nu}^{(1/b)}(z)$ satisfies the recursion relations

$$\begin{aligned} 2\partial_z K_{\nu}^{(b)}(z) &= -K_{\nu+1/b}^{(b)}(z) - K_{\nu-b}^{(b)}(z), \\ 2\nu K_{\nu}^{(b)}(z) &= b^{-1} z K_{\nu+1/b}^{(b)}(z) - b z K_{\nu-b}^{(b)}(z). \end{aligned} \quad (4.43)$$

and behaves for large positive argument as

$$K_{\nu}^{(b)}(2z) \sim \frac{e^{-zM_b}}{\sqrt{z}}, \quad (4.44)$$

where M_b is given by (4.11) with $2M = 1$.

Now, changing in eq. (4.40) the integration variable to $\omega = e^{-2s/(b+b^{-1})}$, we write the disk amplitude with marked boundary as

$$\tilde{W}(\ell) = \frac{1}{\ell} \left(bM^{b^2} K_b^{(b)}(2M\ell) - \frac{t}{b} M^{b-2} K_{1/b}^{(1/b)}(2M\ell) \right). \quad (4.45)$$

5 Relation to Matrix Quantum Mechanics and 2D string theory

5.1 The classical spectral curve of MQM

A non-perturbative formulation of the 2D bosonic string theory is provided by Matrix Quantum Mechanics (MQM) [8–11], see [33] for a standard review on the MQM approach. The idea is to discretise only the gravitational path integral as the ensemble of planar graphs embedded in a one-dimensional continuum, the MQM time. In the scaling limit, the singlet sector of MQM reduces to the dynamics of free fermions in an inverted quadratic potential with a stabilising potential wall far from the top. In the grand canonical ensemble, the cosmological constant is related to the Fermi energy. The maximal value of the Fermi energy, near which the quantum effects prevail, is conventionally set to zero. The thermodynamical

limit corresponds to a Fermi sea filled up to Fermi energy $E_F = -\mu$ and sufficiently far from the maximum. In this regime the dynamics is that of a one-dimensional classical Hamiltonian system with $H = P^2 - X^2$. The individual particles follow classical phase-space trajectories $X = x(E, \tau), P = p(E, \tau)$. The profile of the Fermi sea of the unperturbed system is stationary and follows the trajectory of the particle with maximal energy $E = E_F$, namely $\frac{1}{2}(X^2 - P^2) = \mu$, which also determines the classical spectral curve of the unperturbed MQM. The spectral density is proportional to the discontinuity of the function $P(X)$ on the cut $-\infty < X < \sqrt{2\mu}$,

$$\int_{H(P,X) \leq -\mu} dP \wedge dX = \int_{-\infty}^{-\sqrt{2\mu}} dX \rho(X), \quad \rho(X) = P(X) = \sqrt{X^2 - 2\mu}. \quad (5.1)$$

- *Integrable perturbations by momentum modes.* The MQM is known to be solvable in a nontrivial, time-dependent background generated by a finite tachyon source. Dijkgraaf, Moore and Plesser [14] showed that when the allowed momenta form a lattice as in the case of the compactified Euclidean theory, the perturbation exhibits the Toda integrable structure. Toda integrability was exploited to investigate different aspects of the 2D bosonic string – winding mode [12] and momentum mode [13, 15, 57] condensates as well as non-perturbative effects due to sine-Liouville instantons [16, 17, 58]. The explicit construction of Toda flows with a constraint (string equation) is summarised in [35].

The Toda flows take a simpler form in the chiral representation [13, 57]

$$X_{\pm} = \frac{X \pm P}{\sqrt{2}} \quad (5.2)$$

where the Hamiltonian $H = X_+ X_-$ is diagonalised by Fourier transformation. The sine-Liouville perturbation is then introduced by requiring that the wave functions behave at $X_{\pm} \rightarrow \infty$ as exponentials of $t_{\pm 1} X_{\pm}^{1/R}$. The grand partition function of the theory at finite temperature with $\beta = 2\pi R$ obeys, as a function of t_1, t_{-1} and μ , Toda equation which, together with the string equation, determines the susceptibility $\chi = \partial_{\mu}^2 \log \mathcal{F}_0$ in the thermodynamical limit through the equation of state

$$\mu = e^{-\chi/R} - \frac{1-R}{R} t_1 t_{-1} e^{-\frac{1-R}{R} \chi/R}, \quad R > R_{\text{BKT}} = 1/2. \quad (5.3)$$

The restriction $R > 1/2$ comes from the requirement that the perturbation is relevant. The deformed profile of the Fermi sea is the classical phase-space trajectory for $E = -\mu$,

$$X_{\pm} = x_{\pm}(\tau), \quad x_{\pm}(\tau) = e^{-\chi/2R} e^{\pm\tau} + t_{\mp 1} e^{-\frac{1-R}{R} \chi/2R} e^{\mp \frac{1-R}{R} \tau}. \quad (5.4)$$

For real τ , this is a section of a complex curve where both variables X_+ and X_- are taken real. The spectral curve depends only on the product $t = t_1 t_{-1}$ because the dependence on t_1/t_{-1} can be eliminated by rescaling X_{\pm} . The spectral density $\rho(X)$ of the perturbed model is given in parametric form as $\rho \sim x_+(\tau) - x_-(\tau)$, $X \sim x_+(\tau) + x_-(\tau)$.

- *Integrable perturbations by winding modes.* The sine-Liouville perturbation in the T-dual theory is achieved by imposing $U(N)$ -twisted periodicity in time which effectively

introduces a condensate of winding modes [12, 59, 60]. The perturbation is relevant for $R < \tilde{R}_{\text{BKT}} = 2$. The resulting integral over the eigenvalues of the twisting matrix, first obtained (for the unperturbed theory) by Bulatov and Kazakov [61], resembles the eigenvalue integral (3.14) but with the unit circle as integration contour accompanied by a prescription for surrounding the poles.

The unitary matrix integral can be mapped to free fermions. In the unperturbed theory, the classical fermionic trajectories are given by a section of the complex curve $Z\bar{Z} = \mu$ where the variables Z and \bar{Z} are taken to be complex conjugated to each other.

Perturbations by winding modes also satisfy Toda hierarchy [12] accompanied by a constraint (string equation) for which the Lax operators were constructed in [60]. The partition function $\mathcal{Z} = \exp(\mathcal{F}/\hbar^2)$ perturbed by a condensate of the two lowest winding modes with couplings t_1 and \bar{t}_1 satisfies Toda equation

$$\frac{\partial}{\partial t_1} \frac{\partial}{\partial \bar{t}_1} \mathcal{F}(\mu) + \exp\left(\frac{1}{\hbar^2} [\mathcal{F}(\mu + i\hbar) + \mathcal{F}(\mu - i\hbar) - 2\mathcal{F}(\mu)]\right) = 0 \quad (5.5)$$

with boundary condition for $t_1 \bar{t}_1 = 0$

$$\mathcal{F}(\mu) = -\frac{1}{2} R \mu^2 \log \mu - \hbar^2 \frac{R+R^{-1}}{24} \log \mu + \mathcal{O}(\hbar^2). \quad (5.6)$$

In the thermodynamical (dispersionless) limit $\hbar \rightarrow 0$, the solution for the susceptibility $\chi = \partial_\mu^2 \mathcal{F}$

$$\mu = e^{-\chi/R} - (R-1)t_1 \bar{t}_1 e^{(1-R)\chi/R}, \quad R < 2. \quad (5.7)$$

The classical fermionic phase-space trajectories are given in parametric form by $Z = z(\omega)$, $\bar{Z} = \bar{z}(\omega)$, where ω is a unimodular parameter and

$$\begin{aligned} z &= e^{-\frac{1}{2}\chi} \omega (1 + \bar{t}_1 e^{\frac{2-R}{2R}\chi} \omega^{-1})^R \\ \bar{z} &= e^{-\frac{1}{2}\chi} \omega^{-1} (1 + t_1 e^{\frac{2-R}{2R}\chi} \omega)^R. \end{aligned} \quad (5.8)$$

This spectral curve appears also in another realisation of MQM as a normal matrix model [62].

5.2 7vMM versus MQM

◦ Condensate of momentum modes

Let us show that the MQM with momentum-mode perturbation and the 7-vertex matrix model have the same spectral curve. By a linear change of the parameter, $s = -\frac{\tau}{\lambda+1} - \frac{\lambda}{1-\lambda^2} \log(M)$, the spectral curve of the vertex matrix model, eq. (4.18), takes a form very similar to (5.4)

$$\begin{aligned} x(\tau) &= -e^\tau M^{\frac{1}{1-\lambda}} + e^{\frac{1-\lambda}{1+\lambda}\tau} M^{\frac{1}{1+\lambda}}, \\ y(\tau) &= e^\tau M^{\frac{1}{1-\lambda}} - t e^{\frac{1-\lambda}{1+\lambda}\tau} M^{\frac{1}{1+\lambda}}. \end{aligned} \quad (5.9)$$

The two curves become identical upon setting

$$\begin{aligned} X_+(\tau) &= y(\tau), \quad X_-(\tau) = -x(\tau), \quad t_{-1} = -1, \\ t_1 &= -t, \quad R = \frac{1}{2}(1 + \lambda), \quad e^\chi = M^{\frac{1+\lambda}{1-\lambda}}. \end{aligned} \quad (5.10)$$

Furthermore the equations of state (5.3) and (1.7) match if

$$\mu|_{7\text{vMM}} = R\mu|_{\text{MQM}}, \quad uR = \chi/R. \quad (5.11)$$

Integrating twice, we conclude that in the interval $1/2 < R < 1$ the free energies of the 7vMM and the MQM are related by T-duality.

Expanding both sides of (5.11) in t , we conclude that the correlation functions of the thermal operator in the loop gas model and the correlation functions of the operator creating a pair of tachyons with momenta $p = \pm 1/R$ in MQM are the same. On the other hand, the boundary observables in the two theories are obviously different. For instance, in MQM the dimension of the boundary is half of the dimension of the bulk while in the 7vMM, as we have seen, the boundary has anomalous dimension both in the dilute and in the dense phases.

Another difference is that 7vMM is defined on the interval $\frac{1}{2} < R < 1$ while MQM with a momentum mode condensate is defined for $\frac{1}{2} < R < \infty$. In the Minkowskian picture of MQM, both regimes $\frac{1}{2} < R < 1$ and $1 < R < \infty$ represent time-dependant backgrounds, with the correlation functions of exponential fields interpreted in terms of multiple scattering of massless tachyons off the ‘‘Liouville wall’’. However, the physics in the two regimes is different. When $R > 1$, the two chiral sectors of incoming and outgoing tachyons decouple at infinity and the tachyon scattering is well defined. We have a ‘‘regular’’ background which can be interpreted in terms of multiple tachyon states reflected from a time-dependent, but always time-like, Liouville wall. On the other hand, if $\frac{1}{2} < R < 1$, the Liouville wall becomes at some moment space-like and the outgoing tachyons can no longer be defined. In [63], see also [64], an elaborate physical picture was put forward in which tachyons emitted by the accelerating Liouville wall get eventually absorbed by it.

It would be very interesting to understand how this intricate physics is perceived from the point of view of 7vMM. In the end, the same branched cut which spoils the standard tachyon scattering interpretation appears as condensation of eigenvalues of the 6vMM. The fact that the spectral curve has two different singular points (the infinite points of the domains \mathbb{C}_+ and \mathbb{C}_-) suggests that the asymptotic space for the tachyon scattering should be a direct sum of two sectors and that the scattering matrix is not diagonal.

More specifically, the wave functions, which are the bulk one-point functions on the disk in the ℓ -representation [65, 66], can be expressed in the case of the 7vMM in terms of the generalised Bessel-K function (4.42). The scattering off the Liouville wall of asymptotic states with momenta $\sim i\nu$ is encoded in the small- z expansion

$$\begin{aligned} K_\nu^{(b)}(2z) &= -\frac{1}{2} \sum_{n=0}^{\infty} C_n(\nu, b) z^{b\nu+(1+b^2)n} - \frac{1}{2} \sum_{n=0}^{\infty} C_n(-\nu, 1/b) z^{-\nu/b+(1+b^{-2})n} \\ &= \frac{1}{2} b \Gamma(-b\nu) z^{b\nu} + \frac{1}{2} \frac{\Gamma\left(\frac{\nu}{b}\right) z^{-\frac{\nu}{b}}}{b} + \dots, \quad C_n(\nu, b) = (-1)^n \frac{b \Gamma(-b^2 n - b\nu)}{n!}. \end{aligned} \quad (5.12)$$

The asymptotic space is a direct sum of two sectors related by $b \leftrightarrow 1/b$. The map $b \rightarrow 1/b$ exchanges the compactification circles at the two endpoints of the gravitational massless flow:

$$R_{\text{UV}}^{\text{SL}} = \frac{1+\lambda}{2} = \frac{b^{-1}}{b+b^{-1}} \quad \leftrightarrow \quad \frac{b}{b+b^{-1}} = \frac{1-\lambda}{2} = R_{\text{IR}}^{\text{SL}} \quad (5.13)$$

For imaginary ν , the two lowest terms of the expansion represent incoming and outgoing particles belonging to different sectors of the asymptotic space. A first sight, the momentum is not conserved by the scattering, but actually it is conserved because in the two sectors the boundary length depends differently on the constant Liouville mode, see the discussion after eq. (4.37):

$$\begin{aligned} \ell &= e^{\frac{1+\lambda}{2}\phi} = e^{b^{-1}\ell/(b+b^{-1})} && \text{(dense phase)} \\ \ell &= e^{\frac{1-\lambda}{2}\phi} = e^{b\ell/(b+b^{-1})} && \text{(dilute phase).} \end{aligned} \quad (5.14)$$

◦ *Condensate of winding modes*

Now we turn to the case of perturbations by winding modes. The equation of state (5.7) becomes identical to the equation of state (4.32) in the 7vMM upon replacing

$$R \rightarrow \frac{2}{1+\lambda}, \quad \chi \rightarrow u, \quad t_1 \bar{t}_1 \rightarrow t \quad (1 < R < 2). \quad (5.15)$$

In [12], it was suggested that MQM perturbed by strong winding mode condensate might provide a matrix model for the Euclidean black hole. The pure sine-Liouville theory dual to the Euclidean cigar background [3, 4] should be represented by the vicinity of the critical point $t \rightarrow -\infty$ of the equation of state (5.7). This critical point cannot be achieved by simply setting $\mu = 0$ in (5.7) because by doing that we miss the logarithm in μ and obtain only the uninteresting analytic in μ part of the free energy on the rhs of (4.33).

Another subtle point which surfaces from our analysis of the 6vMM is that the strong perturbation by vortex modes modifies the compactification radius of the asymptotic target space. The radius $\bar{R} = R_{t \rightarrow -\infty}$ is related to the radius $R = R_{t \rightarrow 0}$ by (2.12) after T-duality: $1/\bar{R} = 1 - 1/R$. As the original radius must be in the interval $1 < R < 2$, the radius with strong vortex condensate belongs to the interval $2 < \bar{R} < \infty$ which does not include the radius $R = 3/2$ where the equivalence with the cigar coset model is expected.

6 Discussion

In this paper we proposed a microscopic realisation of the sine-Liouville gravity based on a “dilute” vertex model on a dynamical lattice which represents a one-parameter generalisation of the six-vertex model considered earlier. We extracted the phase diagram of the theory from the classical spectral curve of the dual large- N matrix model and gave a QFT interpretation of the critical points, guided by the phase diagram of the sine-Gordon model on a flat surface. In particular, we identified the gravitational equivalent of the massless flow in the sine-Gordon model with imaginary coupling constant. We conclude with several remarks.

◦ If the coupling constants $t_{\pm 1}$ in (5.3) are identified (up to a normalisation) with μ_{\pm} in the worldsheet action (2.10), the worldsheet theory for the point $t_+ = t_- = 0$ is a massless free boson coupled to Liouville gravity. On the other hand, by the correspondence (5.10), the worldsheet theory for the 7vMM at $t = 0$ is defined by the UV action (2.10) with $\mu_+ = 0$ and $\mu_- \neq 0$. Concerning the bulk observables, the two worldsheet theories are identical because of the charge conservation, but the two theories can have different boundary observables. In the unperturbed MQM, the boundary conditions are imposed independently on the Liouville field and on the free boson and are hence of FZZT [67, 68] type. The boundary cosmological constant is coupled to the area of the world sheet via the Liouville interaction $\mu_B e^{\phi}$. On the other hand, in the 7vMM, the disk partition function for $t \rightarrow 0$ is given by the first term on the rhs of (4.45) with $M \sim \mu^{(1-\lambda)/2}$ and certainly does not correspond to a FZZT brane. The only possibility is that the boundary interaction in the worldsheet theory (2.10) involves both the Liouville and the matter fields.

◦ One can speculate that the boundary term of the sine-Liouville action also has sine-Liouville form. According to (5.14), for $t = 0$ the length element is $dl \sim e^{(1-R)\phi}$. This is the dressing factor for the exponential boundary field $e^{\pm iR\varphi}$. We therefore conjecture that at $t = 0$ the boundary term is of the form

$$\mu_+^B e^{(1-R)\phi} e^{iR\tilde{\varphi}} + \mu_-^B e^{(1-R)\phi} e^{-iR\tilde{\varphi}}, \quad (6.1)$$

where $\tilde{\varphi}$ is the T-dual field of φ , with $x \sim \mu_B = \mu_+^B \mu_-^B$. At the opposite end of the flow, where the Gaussian field is perturbed by an irrelevant sine-Liouville operator, the boundary interaction with the correct scaling of the boundary parameter should again be of the form (6.1), with $R \rightarrow 1 - R$.

◦ For the known solvable models of 2D gravity, such as the $O(n)$, Potts and the ADE on a dynamical lattices, the partition sum for each lattice is a sum over clusters with fugacity depending only on the topology of the cluster and not on the geometry of the lattice. The 6v and the 7v model on dynamical triangulations represent a new type of discrete models of 2D gravity: the gravitational vertex models. In the vertex models on dynamical lattices, the weights of the clusters are not topological but depend on the distribution of the local curvature throughout the lattice. When formulated as height models cf. (3.2), the 6v and the 7v models represent q -deformed dense and dilute versions of the affine \hat{A}_1 height model respectively. It is quite straightforward to formulate the q -deformed $\hat{A}\hat{D}\hat{E}$ models on dynamical surfaces and their dual matrix models.

◦ We studied the near-critical behaviour of the vertex model with a single thermal coupling coupled to the vacancies. This is the simplest of an infinite hierarchy of multicritical points. The multicritical phases and their microscopic construction for $\lambda = 0$ have been studied in [32]. We expect that the continuum CFT for the \hat{A}_n series is again sine-Liouville gravity, eq. (2.10), with $R = \frac{1}{2}n(1 + \lambda)$.

◦ For $\lambda = 0$ ($q = -1$), Alexey Zamolodchikov conjectured [69] that Fredholm determinants of the type (3.16) solve the ‘‘TBA-like’’ integral equations which appear in certain $\mathcal{N} = 2$ supersymmetric theories [70] (see also [71]). This Zamolodchikov conjecture was

later proved by Tracy and Widom [72]. The integral equations are better suited for numerical analysis than the differential equations from Toda hierarchy and it would be interesting whether they can be formulated for general λ . The case $\lambda = 1/6$ was considered in [73].

Acknowledgments

I am grateful to Andre Alves Lima and Mateus da Silva Junca for numerous discussions, and Galen Sotkov for his interest and some important remarks. I thank Sergey Alexandrov, Vladimir Kazakov, David Kutasov and Valentina Petkova for providing useful comments on the draft version of the manuscript.

References

- [1] G. Moore, *Gravitational phase transitions and the sine-gordon model*, [hep-th/9203061](#).
- [2] E. Hsu and D. Kutasov, *The Gravitational Sine-Gordon model*, *Nucl. Phys. B* **396** (1993) 693 [[hep-th/9212023](#)].
- [3] V. Fateev, A. Zamolodchikov and A. Zamolodchikov, “unpublished.”.
- [4] V.A. Fateev, *Integrable deformations of sine-liouville conformal field theory and duality*, *Symmetry, Integrability and Geometry: Methods and Applications* (2017) .
- [5] Y. Hikida and V. Schomerus, *The fzz-duality conjecture — a proof*, *Journal of High Energy Physics* **2009** (2009) 095.
- [6] E. Witten, *String theory and black holes*, *Phys. Rev. D* **44** (1991) 314.
- [7] R. Dijkgraaf, H.L. Verlinde and E.P. Verlinde, *String propagation in a black hole geometry*, *Nucl. Phys. B* **371** (1992) 269.
- [8] V. Kazakov and A. Migdal, *Recent progress in the theory of noncritical strings*, *Nuclear Physics B* **311** (1988) 171.
- [9] E. Brezin, V.A. Kazakov and A.B. Zamolodchikov, *Scaling violation in a field theory of closed strings in one physical dimension* , *Nucl. Phys.* **B338** (1990) 673.
- [10] P. Ginsparg and J. Zinn-Justin, *2d gravity+ 1d matter*, *Physics Letters B* **240** (1990) 333.
- [11] D. Gross and N. Miljkovic, *A nonperturbative solution of d= 1 string theory*, *Physics Letters B* **238** (1990) 217.
- [12] V. Kazakov, I. Kostov and D. Kutasov, *A matrix model for the two-dimensional black hole*, *Nucl. Phys.* **B622** (2002) 141 [[hep-th/0101011](#)].
- [13] S. Alexandrov, V. Kazakov and I. Kostov, *Time-dependent backgrounds of 2D string theory*, *Nucl. Phys.* **B640** (2002) 119 [[hep-th/0205079](#)].
- [14] R. Dijkgraaf, G. Moore and R. Plesser, *The partition function of 2d string theory*, *Nucl.Phys.* **B394** (1993) 356 [[hep-th/9208031](#)].
- [15] S. Alexandrov and V. Kazakov, *Correlators in 2D string theory with vortex condensation*, *Nucl. Phys.* **B610** (2001) 77 [[hep-th/0104094](#)].
- [16] S.Y. Alexandrov and I.K. Kostov, *Time-dependent backgrounds of 2d string theory: Non-perturbative effects*, *JHEP* **0502** (2005) 023 [[hep-th/0412223](#)].

- [17] S. Alexandrov, R. Mahajan and A. Sen, *Instantons in sine-Liouville theory*, *Journal of High Energy Physics* **2024** (2024) 141 [[2311.04969](#)].
- [18] M. Batchelor, B. Nienhuis and S. Warnaar, *Bethe-ansatz results for a solvable $o(n)$ model on the square lattice*, *Physical review letters* **62** (1989) 2425.
- [19] M. Batchelor and H. Blöte, *Conformal anomaly and scaling dimensions of the $o(n)$ model from an exact solution on the honeycomb lattice*, *Physical Review Letters* **61** (1988) 138.
- [20] R. Baxter, *Chromatic polynomials of large triangular lattices*, *Journal of Physics A: Mathematical and General* **20** (1987) 5241.
- [21] R. Baxter, *q colourings of the triangular lattice*, *Journal of Physics A: Mathematical and General* **19** (1986) 2821.
- [22] B. Nienhuis, *Critical behavior of two-dimensional spin models and charge asymmetry in the Coulomb gas*, *J. Stat. Phys.* **34** (1984) 731.
- [23] H. Blöte and M. Nightingale, *Critical behaviour of the two-dimensional potts model with a continuous number of states; a finite size scaling analysis*, *Physica A: Statistical Mechanics and its Applications* **112** (1982) 405.
- [24] P. Fendley, H. Saleur and A.B. Zamolodchikov, *Massless flows. 1. The Sine-Gordon and $O(n)$ models*, *Int. J. Mod. Phys.* **A8** (1993) 5717 [[hep-th/9304050](#)].
- [25] P. Fendley, H. Saleur and A.B. Zamolodchikov, *Massless flows, 2. The Exact S matrix approach*, *Int. J. Mod. Phys.* **A8** (1993) 5751 [[hep-th/9304051](#)].
- [26] A.B. Zamolodchikov, *Thermodynamics of imaginary coupled sine-Gordon: Dense polymer finite size scaling function*, *Phys. Lett.* **B335** (1994) 436.
- [27] I. Kostov, *$O(n)$ vector model on a planar random surface: spectrum of anomalous dimensions*, *Mod. Phys. Lett.* **A4** (1989) 217.
- [28] P.H. Ginsparg, *Matrix models of 2-d gravity*, 1991.
- [29] I. Kostov, *Exact solution of the six-vertex model on a random lattice*, *Nucl. Phys.* **B575** (2000) 513 [[hep-th/9911023](#)].
- [30] P. Zinn-Justin, *The six-vertex model on random lattices*, *Europhys. Lett.* **50** (2000) 15 [[cond-mat/9909250](#)].
- [31] A. Elvey Price and P. Zinn-Justin, *The six-vertex model on random planar maps revisited*, *Journal of Combinatorial Theory, Series A* **196** (2023) 105739.
- [32] I. Kostov and M. Staudacher, *Multicritical phases of the $O(n)$ model on a random lattice*, *Nucl. Phys.* **B384** (1992) 459 [[hep-th/9203030](#)].
- [33] I.R. Klebanov, *String Theory in Two Dimensions*, *ArXiv High Energy Physics - Theory e-prints* (1991) [[arXiv:hep-th/9108019](#)].
- [34] A.A. Lima, I. Kostov and M.D.S. Junca, *work in progress*.
- [35] I. Kostov, *Integrable flows in $c = 1$ string theory*, *J. Phys.* **A36** (2003) 3153 [[hep-th/0208034](#)].
- [36] E. Krätzel, *Integral transformations of bessel type*, in *Generalized Functions and Operational Calculus*, *Proc. Conf. Varna*, pp. 148–155, 1975.

- [37] J.V. José, L.P. Kadanoff, S. Kirkpatrick and D.R. Nelson, *Renormalization, vortices, and symmetry-breaking perturbations in the two-dimensional planar model*, *Phys. Rev. B* **16** (1977) 1217.
- [38] V.G. Knizhnik, A.M. Polyakov and A.B. Zamolodchikov, *Fractal structure of 2d-quantum gravity*, *Mod. Phys. Lett.* **A3** (1988) 819.
- [39] F. David, *Conformal Field Theories Coupled to 2D Gravity in the Conformal Gauge*, *Mod. Phys. Lett.* **A3** (1988) 1651.
- [40] J. Distler and H. Kawai, *Conformal field theory and 2d quantum gravity*, *Nuclear Physics B* **321** (1989) 509.
- [41] F. David, *Planar Diagrams, Two-Dimensional Lattice Gravity and Surface Models*, *Nucl. Phys.* **B257** (1985) 45.
- [42] J. Ambjorn, B. Durhuus and J. Fröhlich, *Diseases of Triangulated Random Surface Models, and Possible Cures*, *Nucl. Phys.* **B257** (1985) 433.
- [43] D. Boulatov, V. Kazakov, I. Kostov and A. Migdal, *Analytical and Numerical Study of the Model of Dynamically Triangulated Random Surfaces*, *Nucl. Phys.* **B275** (1986) 641.
- [44] O. Foda and B. Nienhuis, *The Coulomb gas representation of critical RSOS models on the sphere and on the torus*, *Nucl. Phys.* **B324** (1989) 643.
- [45] I. Kostov, B. Ponsot and D. Serban, *Boundary liouville theory and 2d quantum gravity*, *Nucl.Phys.* **B683** (2004) 309 [[hep-th/0307189](#)].
- [46] M.V. Berry, *Quantal phase factors accompanying adiabatic changes*, *Proceedings of the Royal Society of London. A. Mathematical and Physical Sciences* **392** (1984) 45.
- [47] J.R. Hoppe, *Quantum Theory of a Massless Relativistic Surface and a Two-Dimensional Bound State Problem.*, Ph.D. thesis, Massachusetts Institute of Technology, Jan., 1982.
- [48] V. Kazakov, I. Kostov and N.A. Nekrasov, *D-particles, matrix integrals and KP hierarchy*, *Nucl. Phys.* **B557** (1999) 413 [[hep-th/9810035](#)].
- [49] J. Hoppe, V. Kazakov and I. Kostov, *Dimensionally reduced SYM(4) as solvable matrix quantum mechanics*, *Nucl. Phys.* **B571** (2000) 479 [[hep-th/9907058](#)].
- [50] R. Dijkgraaf and C. Vafa, *A perturbative window into non-perturbative physics*, [hep-th/0208048](#).
- [51] N. Dorey, T.J. Hollowood and S.P. Kumar, *S-duality of the Leigh-Strassler deformation via matrix models*, *Journal of High Energy Physics* **2002** (2002) 003.
- [52] M. Marino, *Spectral Theory and Mirror Symmetry*, *ArXiv e-prints* (2015) [[1506.07757](#)].
- [53] S. Zakany, *Matrix models and eigenfunctions from the Topological String/Spectral Theory correspondence*, Ph.D. thesis, éditeur non identifié, 2019.
- [54] M. Bousquet-Mélou and A.E. Price, *Refined enumeration of planar eulerian orientations*, *arXiv preprint arXiv:2503.15046* (2025) .
- [55] A.M. Mathai and H.J. Haubold, *Mathematical aspects of Krätzel integral and Krätzel transform*, *Mathematics* **8** (2020) .
- [56] A.A. Kabeer and D. Kumar, *Generalized Krätzel functions: an analytic study*, *Fractional Calculus and Applied Analysis* **27** (2024) 799.

- [57] S. Alexandrov, *Matrix Quantum Mechanics and Two-dimensional String Theory in Non-trivial Backgrounds*, Ph.D. thesis, 2003. [hep-th/0311273](#).
- [58] S. Alexandrov, V. Kazakov and D. Kutasov, *Non-perturbative effects in matrix models and D-branes*, *JHEP* **09** (2003) 057 [[hep-th/0306177](#)].
- [59] D.J. Gross and I.R. Klebanov, *Vortices and the nonsinglet sector of the $c = 1$ matrix model*, *Nucl. Phys.* **B354** (1991) 459.
- [60] I. Kostov, *String equation for string theory on a circle*, *Nucl. Phys.* **B624** (2002) 146 [[hep-th/0107247](#)].
- [61] D. Boulatov and V. Kazakov, *One-dimensional string theory with vortices as the upside-down matrix oscillator*, *International Journal of Modern Physics A* **08** (1993) 809.
- [62] S. Alexandrov, V. Kazakov and I. Kostov, *2D string theory as normal matrix model*, *Nucl. Phys.* **B667** (2003) 90 [[hep-th/0302106](#)].
- [63] B. Balthazar, J. Chu and D. Kutasov, *On time-dependent backgrounds in 1+1 dimensional string theory*, 2023.
- [64] S.R. Das, S.D. Hampton and S. Liu, *Superluminal Liouville walls in 2d String Theory and space-like singularities*, [2509.12778](#).
- [65] G.W. Moore, N. Seiberg and M. Staudacher, *From loops to states in 2-D quantum gravity*, *Nucl. Phys.* **B362** (1991) 665.
- [66] G.W. Moore and N. Seiberg, *From loops to fields in 2-D quantum gravity*, *Int. J. Mod. Phys. A* **7** (1992) 2601.
- [67] V. Fateev, A.B. Zamolodchikov and A.B. Zamolodchikov, *Boundary Liouville field theory. I: Boundary state and boundary two-point function*, [hep-th/0001012](#).
- [68] J. Teschner, *Liouville theory revisited*, *Class.Quant.Grav.* **18** (2001) R153 [[hep-th/0104158](#)].
- [69] A.B. Zamolodchikov, *Painleve III and 2-d polymers*, *Nucl. Phys.* **B432** (1994) 427 [[hep-th/9409108](#)].
- [70] S. Cecotti, P. Fendley, K.A. Intriligator and C. Vafa, *A New supersymmetric index*, *Nucl.Phys.* **B386** (1992) 405 [[hep-th/9204102](#)].
- [71] S. Cecotti and C. Vafa, *Topological-antitopological fusion*, *Nucl.Phys.* **B367** (1991) 359.
- [72] C.A. Tracy and H. Widom, *Proofs of two conjectures related to the thermodynamic bethe ansatz*, *Communications in Mathematical Physics* **179** (1996) 667.
- [73] K. Okuyama and S. Zakany, *TBA-like integral equations from quantized mirror curves*, *JHEP* **03** (2016) 101 [[1512.06904](#)].